The valosin-containing protein is implicated in West Nile virus replication and an examination of the pathogenicity of novel WNV strain isolated in Zambia

（ウエストナイルウイルスの複製に関与するバロシン含有タンパク質に関する研究とザンビアで単離されたウエストナイルウイルスの病原性の検索）

Wallaya PHONGPHAEW

CONTENTS

List of Abbreviations

AAA+ ATPase	Adenosine triphosphatase-associated with diverse cellular activities
BBB	Blood brain barrier
BSA	Bovine serum albumin
BSL-3	Biosafety level-3
C6/36	*Aedes albopictus* mosquito cell line
C. univittatus	*Culex univittatus*
DC-SIGN	Dendritic cell-specific intercellular adhesion molecule-3-grabbing non-integrin
DMEM	Dulbecco's modified eagle's medium
DMSO	Dimethyl sulfoxide
dpi	Day post inoculation
EerI	Eeyarestatin I
Eg101	WNV Egypt strain
ER	Endoplasmic Reticulum
ERAD	ER-associated degradation
FBS	Fetal bovine serum
GFP	Green fluorescence protein
h	hour
HAU	Hemagglutination units
HCV	Hepatitis C virus
HEK-293T	Human embryonic kidney-293T
hpi	hour post infection

HRP	Horseradish peroxidase
IBV	Infectious bronchitis virus
IFA	Immunofluorescence assay
IFU	Infectious units
IC	Intracranial
IgG	Immunoglobulin G
IgM	Immunoglobulin M
IP	Intraperitoneal
IL-6	Interleukin-6
JEV	Japanese Encephalitis virus
kb	Kilo base pair
L-SIGN	Liver/lymph node-specific intercellular adhesion molecule-3-grabbing non-integrin
MEM	Minimum essential media
MDBN	3,4-Methylenedioxy-β-nitrostyrene
min	minute
MOI	Multiplicity of infection
MST	Median survival time
MTT	3-(4,5-dimethylthiazol-2-yl)-2,5-diphenyltetrazolium bromide
mRNA	Messenger ribonucleic acid
NA	Mouse neuroblastoma clone NA cell line
NPL4	Nuclear protein localization 4
NRAMP2	Natural-resistance associated macrophage protein 2

NS	Non-structural protein
NY99 6-LP	WNV New York strain
PBS	Phosphate buffered saline
PCR	Polymerase chain reaction
PFU	Plaque forming unit
PV	Poliovirus
qRT-PCR	Quantitative real-time reverse transcription PCR
RNA	Ribonucleic acid
SDS-PAGE	Sodium dodecyl sulfate- polyacrylamide gel electrophoresis
siRNA	Small interfering RNA
SG	Stress granule
SINV	Sindbis virus
SK-N-SH	Human neuroblastoma cell line
TAM	Tyro3, Axl and Mer
TIM	T cell/transmembrane, immunoglobulin and mucin
TBS-T	Tris-buffered saline with Tween 20
TNF-α	Tumor necrosis factor-alpha
UFD1L	Ubiquitin fusion degradation 1-like
USA	United States of America
VCP	Valosin-containing protein
VLP	Virus-like particle
VSV	Vesicular stomatitis virus

WNV	West Nile virus

Preface

West Nile virus (WNV) is a zoonotic pathogen can cause West Nile virus fever and encephalitis in human and several kinds of mammals such as horses and dogs. WNV belongs to the genus *Flavivirus* in the family *Flaviviridae*, and has approximately 11 kb of positive sense single-stranded genomic RNA. The genomic RNA of WNV encodes ten proteins, including three structural proteins and seven non-structural proteins. This virus is transmitted by mosquito bite, especially *Culex* spp., and widely spread to many countries. Wild birds play an important role as a primary vertebrate reservoir of WNV. In 1999, at New York, United States of America (USA), there was major outbreak of WNV strain, NY99 which is a cause of endemic in USA until now. Approved vaccine and specific treatment for WNV infection have not been available yet. Understanding of WNV in several aspects, including pathogenicity, host-virus interaction, host immunological responses and epidemiology would provide the valuable knowledge for development of vaccine and therapeutic agents to prevent and cure for WNV infection.

This thesis consists of two chapters. The first chapter contains the investigation of the role of valosin-containing protein (VCP) in the replication of WNV. The second chapter represents examination of pathogenicity of a novel strain of WNV isolated from captured mosquitoes in the Republic of Zambia.

Chapter I

The valosin-containing protein (VCP) is implicated in West Nile virus replication

Introduction

West Nile virus (WNV) belongs to the genus *Flavivirus* in the family *Flaviviridae* and has an approximately 11 kb positive sense, single-stranded genomic RNA [(+)ssRNA]. The WNV genome encodes three structural proteins (C, prM and E) and seven non-structural proteins (NS1, NS2A, NS2B, NS3, NS4A, NS4B and NS5; Fig. 1) (Brinton, 2014; Knipe et al., 2013). Many species of mammals and birds can be infected by WNV (Dauphin et al., 2004; Egberink et al., 2015; Knipe et al., 2013; Gamino et al., 2016; Kramer and Bernard, 2001; Lichtensteiger et al., 2003; Read et al., 2005) which causes West Nile fever and encephalitis in human and horses (Dauphin et al., 2004; Samuel and Diamond, 2006). WNV was firstly isolated from a Ugandan woman in 1937 (Smithburn. et al., 1940; Knipe et al., 2013), but has now spread widely to many countries (Knipe et al., 2013; Paz, 2015; Troupin and Colpitts, 2016). In the United States, approximately 44,000 cases of WNV infection were reported between 1999 and 2015 (Centers for Disease Control and Prevention, 2016).

WNV attaches to host cells through the interaction of the viral E protein and cellular receptors on the surface of host cells (Knipe et al., 2013). Several attachment receptors of WNV have been reported, including laminin receptor (Bogachek et al., 2010; Perera-Lecoin et al., 2014; Zaitsev et al., 2014; Zidane et al., 2013), TIM (T cell/transmembrane, immunoglobulin and mucin) and TAM (Tyro3, Axl and Mer) families (Carnec et al., 2016; Morizono and Chen, 2014; Perera-Lecoin et al., 2014), DC-SIGN/L-SIGN (dendritic cell-specific intercellular adhesion molecule-3-grabbing

non-integrin/ liver or lymph node- specific intercellular adhesion molecule-3-grabbing non-integrin) (Davis et al., 2006; Denizot et al., 2012; Martina et al., 2008; Shimojima et al., 2014) and integrin αvβ3 (Bogachek et al., 2010; Knipe et al., 2013; Perera-Lecoin et al., 2014; Smit et al., 2011; Zaitsev et al., 2014). Following attachment, the virus is then internalized into the cytoplasm *via* clathrin-mediated endocytosis (Brinton, 2014; Chu and Ng, 2004; Knipe et al., 2013). WNV particles are delivered to early or intermediate endosomes, which mature into late endosomes, following a conformational change of the viral E protein dimer triggered by the acidic environment in late endosomes. Membrane fusion between viral particles and endosomal membranes then occurs and, thereafter, WNV genomic RNA is released into the cytosol, with subsequent translation and replication (Chu et al., 2006; Chu and Ng, 2004; Knipe et al., 2013; Heinz and Allison, 2000; Smit et al., 2011). Host cell membrane rearrangements are induced during replication of flaviviruses, including WNV, to coordinate the processes of genomic RNA replication and virus assembly. Viral genomic RNA replication is thought to occur in endoplasmic reticulum (ER) membrane-derived vesicles (in structures termed vesicle pockets) (Gillespie et al., 2010; Kaufusi et al., 2014; Welsch et al., 2009). Encapsidation of nascent viral genomic RNA is achieved by capsid protein and budding into the ER yielding a viral envelope coated with prM and E proteins (Brinton, 2014; Knipe et al., 2013; Suthar et al., 2013; Welsch et al., 2009). The immature virions are transported *via* the host secretory pathway and virion maturation then occurs in the acidic compartments of the Golgi by cleavage of the prM protein by a furin-like protease (Plevka et al., 2014; Roby et al., 2015; Yu et al., 2008). Mature virions are then released from the infected cells through exocytosis (Knipe et al., 2013; Samuel and Diamond, 2006). It has been reported that several cellular pathways and host factors

are involved in WNV infection (Ambrose and Mackenzie, 2011; Brinton, 2014; Chahar et al., 2013; Chu and Ng, 2004; Courtney et al., 2012; Fernandez-Garcia et al., 2011; Knipe et al., 2013; Gilfoy et al., 2009; Kobayashi et al., 2016; Krishnan et al., 2008; Ma et al., 2015); however, the role of valosin-containing protein (VCP) has remained controversial.

VCP, also known as CDC48 in *Saccharomyces cerevisiae*, is well conserved among eukaryotes with orthologues in archaea, protozoa, insects and plants (Meyer et al., 2012; Wolf and Stolz, 2012), and is classified as a member of the type II AAA^+ ATPase (adenosine triphosphatase-associated with diverse cellular activities) family (Koller and Brownstein, 1987; Pye et al., 2006; Stolz et al., 2011; Wolf and Stolz, 2012; Xia et al., 2016). VCP is a homohexameric complex composed of six protomers organized as two concentric-rings with a central pore. VCP conformational changes driven by adenosine triphosphate hydrolysis acts as a chaperone in protein homeostasis systems which include ER-associated degradation (ERAD) (Wolf and Stolz, 2012; Xia et al., 2016; Zhong and Pittman, 2006) and mitochondria-associated degradation and autophagy (Bug and Meyer, 2012; Dargemont and Ossareh-Nazari, 2012; Xia et al., 2016; Yamanaka et al., 2012). These systems prevent accumulation of misfolded-proteins and turnover of certain proteins. Recently, a role of VCP in the disassembly of stress granules (SGs) has also been reported (Buchan et al., 2013; Seguin et al., 2014). Generally, after removal of stress stimuli, SGs are disassembled by VCP and mRNA in the SGs could be restored allowing mRNA translation to proceed. Otherwise, depletion of VCP causes persistence of SGs leading to blockage of mRNA restoration and an arrest of mRNA translation (Buchan et al., 2013). It has also been reported that VCP is involved in chromatin-associated degradation and several nuclear substrates of VCP have been described (Maric et al., 2014; Verma et

al., 2011; Wilcox and Laney, 2009). Furthermore, VCP also participates in membrane fusion and vesicular trafficking events (Bug and Meyer, 2012; Meyer et al., 2012; Ramanathan and Ye, 2012; Ritz et al., 2011; Xia et al., 2016). VCP binds to endocytic components, and silencing of VCP leads to a failure of maturation and enlargement of the early endosome (Ramanathan and Ye, 2012).

Interestingly, VCP has also been implicated in the life cycle of several (+) ssRNA viruses. It has been previously reported that VCP facilitates the replication of poliovirus (PV) (Arita et al., 2012). Depletion of VCP caused a reduction of PV infection, whereas, a mutant PV, which has a secretion inhibition-negative phenotype, increases the affinity of binding to VCP and resists VCP-knockdown compared to wild-type PV, suggesting that VCP may play a role in PV replication through cellular secretion pathways. In addition, other roles for VCP have been described in other picornaviruses. Although VCP-knockdown strongly inhibits PV infection, inhibition of VCP does not affect the replication of Coxsackievirus B3 (Arita et al., 2012), which is also a member of the same genus *Enterovirus*. In contrast, replication of Aichivirus A, genus *Kobuvirus*, another member of family *Picornaviridae*, is enhanced when VCP is depleted (Arita et al., 2012).

A relationship between VCP and Sindbis virus (SINV) replication has also been reported (Panda et al., 2013). VCP is involved in trafficking of the entry receptor of SINV, which is the natural resistance-associated macrophage protein 2 (NRAMP2). Deficiency of VCP suppresses SINV replication through alteration of trafficking routes of NRAMP2 leading to degradation of NRAMP2 by lysosomes.

Studies of infectious bronchitis virus (IBV), family *Coronaviridae*, have suggested that VCP is engaged in the internalization steps of IBV (Wong et al., 2015). VCP-knockdown using siRNA, resulted in accumulation of IBV particles in early

endosomes as maturation of the endosome, and acidification of endosome was disrupted. Failure of the acidification of virus-containing endosomes inhibited fusion between the virus envelope and endosomal membrane and prevented IBV exit from the endosomes to the cytosol (Wong et al., 2015).

In the present study, VCP was investigated whether it is involved in WNV infection. Specifically, VCP inhibitors and siRNA knockdown were employed to elucidate a potential role of VCP in WNV replication.

Fig. 1

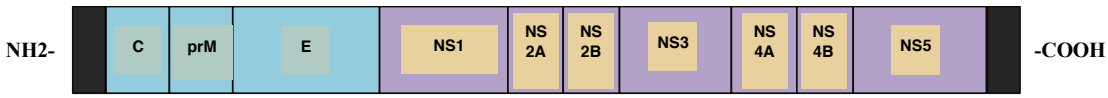

Schematic representation of WNV genomic RNA

Materials and Methods

Cell and viruses

Human cervical adenocarcinoma cells, HeLa, were grown in Dulbecco's modified eagle's medium (DMEM) supplemented with 10% fetal bovine serum (FBS) and 2 mM L-glutamine. Human embryonic kidney cells, HEK293T, were grown in high glucose DMEM supplemented with 110 mg/L sodium pyruvate, 2 mM L-glutamine and 5% FBS. African green monkey kidney cells, Vero, were grown with Minimum essential media (MEM) supplemented with 5% FBS and 2 mM L-glutamine. Human neuroblastoma cells, SK-N-SH, were grown with MEM supplemented with 10% FBS and 2 mM L-glutamine. Cells were grown at 37 °C with 5% supplemented CO_2. The mosquito cell line, *Aedes albopictus* clone C6/36, were grown in MEM supplemented with 10% FBS, 1% non-essential amino acid and 2 mM L-glutamine at 28 °C. WNV NY99 6-LP was propagated in C6/36 at 28 °C. WNV-NY99 6-LP was kindly provided by Dr. Takashima (Laboratory of Public Health, Graduate school of Veterinary Medicine, Hokkaido University, Sapporo, Japan) (Hasebe et al., 2010; Shirato et al., 2004a; Shirato et al., 2004b). Viral titer was measured by plaque assay and stock of viruses were stored at -80 °C until use. All experiments with WNV were performed in the Biosafety level-3 (BSL-3) facility at the Research Center for Zoonosis Control, Hokkaido University in accordance with the institutional guidelines. Recombinant-vesicular stomatitis virus (VSV) was provided by Dr. Takada (Research Center for Zoonosis Control, Hokkaido University) (Takada et al., 2007).

MTT assay

HeLa cells were treated with 5, 10 and 20 μM of Eeyarestatin I (EerI) (Sigma Aldrich, St. Louis, MO) (Wang et al., 2008; Wang et al., 2010) or 12.5, 25 and 50 μM of 3,4-Methylenedioxy-β-nitrostyrene (MDBN) (Abcam, Cambridge, UK) (Chou and Deshaies, 2011) and incubated at 37 °C for 24 h. Thereafter, the treated cells were examined by an MTT assay, following addition of 3-(4,5-dimethylthiazol-2-yl)-2,5-diphenyltetrazolium bromide (MTT) and incubated at 37 °C for 1 h, then addition of solubilization solution [10% Triton-X 100 in acidic isopropanol (0.1N HCl)] and incubation at room temperature with shaking for 30 min. Absorbance values were measured at 570 nm and 630 nm using the Model 680 microplate reader (Bio-rad, Hercules, CA).

Plaque assay

Virus suspensions were diluted in a series of 10-fold dilutions and inoculated onto monolayers of Vero cells. The WNV-inoculated Vero cells were grown in MEM containing 1.25% methyl cellulose, 5% FBS and 2 mM L-glutamine at 37 °C for 4 days. Thereafter, fixation was performed using 10% formalin for 10 min at room temperature. The fixed cells were stained with 1% crystal violet in 70% ethanol for 30 min. The number of plaques was counted and the virus titer was determined in plaque forming unit per milliliter (PFU/ml).

Immunofluorescence assay (IFA)

The WNV-infected cells grown on coverslips were fixed at various times after infection. The infected cells were fixed in 4% paraformaldehyde for 10 min and permeabilized using 0.1% Triton X-100 for 5 min at room temperature. Blocking was

performed with 1% bovine serum albumin (BSA) for 30 min before incubation with primary antibody. The cells were incubated with a primary antibody (rabbit anti-JEV serum; 1:1,500) (Kimura et al., 1994; Kobayashi et al., 2012) that has cross-reactivity with the WNV antigens at 4 °C overnight, followed by incubation with Alexa Fluor 488-conjugated secondary antibody against rabbit IgG (1:2,000; Life technologies, Rockville, MD) for 1 h at room temperature. The cells were washed three times with phosphate buffered saline (PBS) before fluorescence microscopy examination. The cells were visualized using an inverted fluorescence microscope (IX70, Olympus, Tokyo, Japan) and images were processed using DP manager software (Olympus).

Immunoblotting analysis

Cell samples were harvested at the indicated time points using TNE lysis buffer [1% Triton X-100, 10 mM Tris-HCl (pH 7.5), 150 mM NaCl, 5 mM EDTA, 10% glycerol] and centrifuged at 17,800 x *g* at 4 °C for 20 min. Only supernatants were collected and mixed with Sodium dodecyl sulfate-Polyacrylamide gel electrophoresis (SDS-PAGE) sample buffer [0.1 M Tris-HCl (pH 6.8), 3.3% SDS, 11% glycerol]. The samples were separated by 8% PAGE and then transferred to a polyvinylidene difluoride filter (Merck Millipore, Billerica, MA). The filters were blocked with 5% skimmed milk for 30 min. The filters were incubated with each primary antibody, including mouse anti-VCP antibody (1:2,000; Abcam), mouse anti-envelope protein of West Nile/Kunjin virus (1:1,000; Merck Millipore), rabbit anti-NS3 serum (1:1,000), which was prepared from a rabbit immunized by twice intravenous inoculations of synthetic peptides of NS3 (CEREKVYTMDGEYRLRGEER), and mouse anti-actin (1:1,000; Merck Millipore). Thereafter, the filters were incubated with secondary antibody, goat anti-mouse IgG

antibody conjugated with horseradish peroxidase (HRP) at 1:10,000 dilution (Biosource International, Camarillo, CA) and washed with TBS [50 mM Tris-HCl (pH 7.5), 150 mM NaCl,] containing 0.05% Tween 20 (TBS-T) three times. Chemiluminescence was detected by Immobilon Western HRP Substrate (Merck Millipore) and visualized with VersaDoc 5000MP (Bio-Rad), and images were analyzed using Quantity One software (Bio-Rad).

WNV inoculation in the presence of VCP inhibitors

Based on the results of MTT assays, the optimal concentration of EerI (2.5 and 5 μM) and MDBN (6.25 and 12.5 μM) without cytotoxicity in HeLa cells were determined. Multiplicity of infection (MOI) of 1 of WNV NY99 6-LP strain (MOI of 1 of WNV causing 100% infection of Vero cells) was inoculated into HeLa cells. After 1 h of incubation at 37 °C with rocking, the inocula were removed. Suspensions of either EerI or MDBN diluted in normal cultured medium were added to the WNV-inoculated cells and incubated at 37 °C for 24 h. Thereafter, the inoculated-cells and the supernatants were prepared for IFA, plaque assay and immunoblotting analysis to measure the number of WNV-infected cells, production of infectious WNV and expression of WNV proteins, respectively.

VCP knockdown

The endogenous VCP was inhibited using small interfering RNA (siRNA). HeLa cells (2 x 10^4 cells in 250 μl medium per well) in 48-well plates were transfected with 5 nM of each siRNA targeting VCP, no. (1), (2) and (3), which have the sequences 5′-GAAUAGAGUUGUUCGGAAUTT-3′, 5′-GAACCGUC CCAAUCGGUUATT-3′, and 5′-GGCUCGUGGAGGUAACAUUTT-3′ (Thermo

Fisher Scientific, Waltham, MA), respectively, using lipofectamine RNAiMAX transfection reagent (Thermo Fisher Scientific) according to the manufacturer's instructions. The transfected cells were incubated at 37 ℃ for 48 h. The expression level of VCP was evaluated using immunoblotting.

WNV inoculation in siRNA-treated cells

At 48 h post transfection with either siRNA against VCP or control siRNA (Catalogue No: 439084, Thermo Fisher Scientific), HeLa cells were inoculated with WNV NY99 6-LP strain (MOI=1; MOI of 1 of WNV causing 100% infection of Vero cells) and incubated at 37 ℃ for 1 h with rotation. Thereafter, supernatants of the cells were removed, and normal HeLa culture medium was added to the cells and incubated at 37 ℃ for 12, 24 and 48 h. The inoculated cells and the supernatants were prepared for IFA, plaque assay and immunoblotting analysis. To investigate the role of VCP at the early stages of the WNV replicative cycle, the siRNA-transfected cells were inoculated with WNV as described above. After inoculation of WNV, cells were incubated on ice for 1 h, and then washed with PBS five times. The cells were then placed at 37 ℃ and incubated for 1 h. Thereafter, the inoculated-cells were harvested using trypsin. The detached cells from cell culture plates were centrifuged at 1,500 x *g* for 3 min. After removal of supernatants, total RNA was extracted from cell pellets using Trizol (Thermo Fisher Scientific). Extracted total RNAs were analyzed for WNV genome using quantitative real-time reverse transcription PCR (qRT-PCR) analysis.

Recombinant-VSV inoculation in siRNA-treated cells

It has been previously reported that VCP knockdown did not affect VSV infection (Panda et al., 2013). Therefore, control experiments using recombinant-VSV were performed. Recombinant-VSV encoding green fluorescent protein (GFP) was kindly provided by Dr. Takada (Hokkaido University) (Takada et al., 2007). The recombinant-VSV was inoculated into HeLa cells transfected with either siRNA against VCP or control siRNA. The cells were incubated at 37 °C with rotation for 1 h. Thereafter, supernatants of the cells were removed, normal growth media was added to the cells and incubated at 37 °C for 8 h. The percentage positivity following recombinant-VSV infection was measured by counting the number of GFP-positive cells using an inverted fluorescence microscope (IX70, Olympus).

Production of WNV virus-like particles (WNV-VLPs)

WNV-VLPs with reporter DsRed protein were produced following transfection. Three plasmid vectors carrying WNV sequences: pCMV-WNrep-DsRed, pCMV-SVP and pCSXN-C were transfected into HEK293T cells using lipofectamine 2000 (Thermo Fisher Scientific). These plasmids were constructed as follows. A pCMV-WNrep-DsRed encoding WNV replicon cDNA contains non-structural proteins (NS1-NS5) and lacks almost all of structural proteins (C, prM and E) replaced with DsRed protein. The 3′-terminus of the WNV genome was accomplished by containing sequences enabling ribozyme-mediated post-transcriptional cleavage of the RNA (Kobayashi et al., 2017). The fragment of prM-E was amplified by PCR from pCAGGS-C-prM-E, which was a gift from Dr. Takashima (Hokkaido University) (Takahashi et al., 2009) as a template, and subcloned into the pCMV vector, and the plasmid was named pCMV-SVP. For the

pCSXN-C, the C fragment with restriction sequences of Xho I and Not I (Takara Bio, Kyoto, Japan) were amplified by PCR and inserted into pCSXN-flag which was generated from pCMV-myc (Clontech Laboratories, Mountain View, CA) as previously described (Kobayashi et al., 2013), using Xho I and Not I restriction sites. The plasmid was named as pCXSN-C. The transfected cells were incubated at 37 °C for 72 h. The supernatants from transfected cells were collected and filtered through a 0.45 μm filter (Sigma Aldrich). The WNV-VLPs were concentrated by ultracentifugation at 4 °C, 68,000 x *g* for 2 h. The supernatant was discarded and only the pellet was collected after ultracentrifugation. The pellet was resuspended with DMEM with 10% FBS and 2 mM L-glutamine, and the titers of WNV-VLPs were measured by hemagglutination assay as previously described (Makino et al., 2014). The titer of VLPs was calculated as hemagglutination units (HAU)/50 μl based on the highest dilution of VLP suspension causing agglutination of chicken red blood cells.

Inoculation of WNV-VLPs in VCP-knockdown HeLa cells

WNV-VLPs (16 HAU/50 μl) were inoculated into siRNA-treated HeLa cells 48 h post transfection. After 1 h incubation at 37 °C, the inocula were discarded and DMEM with 10% FBS and 2 mM L-glutamine was added and incubated for 72 h. Comparison of the quantity of WNV-RNA between VCP-knockdown and control was determined using qRT-PCR.

WNV-VLP production and transfection of pCMV-WNrep-DsRed to siRNA-treated HeLa cells

Plasmid transfection to generate WNV-VLPs has been reported to investigate the role of VCP in the late steps of viral life cycle, from genome replication to virus

release (Kobayashi et al., 2016). The results obtained employing the plasmid-encoded VLPs would not be attributable to early steps of WNV infection, including attachment and entry. WNV-VLPs were used to investigate the role of VCP in distinct steps (early and genome replication steps) of WNV infection cycle. At 24 h after siRNA transfection, the plasmid set (pCMV-WNrep-DsRed, pCMV-SVP and pCSXN-C) was transfected into siRNA-treated HeLa cells using FuGENE HD (Promega, Madison, WI). The plasmid transfected-cells were incubated at 37 °C for 72 h. Thereafter, the supernatants from transfected cells were collected and inoculated onto Vero cells monolayers in 10-fold serial dilutions. WNV-VLP titer was calculated as infectious units (IFU)/ml based on the total number of DsRed-positive cells (Fig. 9C).

To investigate the role of VCP in WNV genomic RNA replication, only pCMV-WNrep-DsRed (Kobayashi et al., 2017) was transfected into the siRNA-treated cells. The procedure and time of transfection are similar to plasmid transfection for VLP production. After 72 h incubation, the total RNAs were extracted and prepared for qRT-PCR.

Real-time reverse transcription-PCR (qRT-PCR)

Total RNA was isolated by Trizol and chloroform according to the manufacturer's protocol. The RNA samples were treated with DNase I (Thermo Fisher Scientific) to remove genomic DNA. qRT-PCR was performed with a Brilliant III Ultra-Fast qRT-PCR master mix (Agilent Technologies, Santa Clara, CA) following the manufacturer's protocol. The oligonucleotide primers and fluorescent probe targeting the 3′UTR of WNV, 5′-AAGTTGAGTAGACGGTGCTG-3′ and 5′-AGACGGTTCTGAGGGCTTAC-3′, WNV probe, FAM-5′-GCTCAACCCCAGGA-GGACTGG-3′-BHQ, were used for detection of WNV-RNA. A TaqMan Gene

expression assays kit corresponding to human β-actin (Thermo Fisher Scientific) was used as an endogenous control. The expression level of viral RNA was normalized to the expression of human β-actin.

Statistical analysis

The statistical significance was calculated using one-way ANOVA.

Results

WNV infection is inhibited in the presence of VCP inhibitors

To determine if VCP is involved in WNV infection, the effect of VCP inhibitors, both EerI (Wang et al., 2008; Wang et al., 2010) and MDBN (Chou and Deshaies, 2011) at concentrations without cytotoxicity were assayed in WNV infection. The cytotoxicity of either EerI or MDBN treatment in HeLa cells was examined using an MTT assay (Fig. 2). Each VCP inhibitor was added to HeLa cells at 1 hour post infection (hpi) with WNV and WNV-inoculated cells and cultured supernatants were harvested at 24 hpi. The number of WNV-infected cells was examined by IFA, and this revealed that the number of WNV-infected cells was significantly decreased in a dose-dependent manner in the presence of either EerI or MDBN (Fig. 3A and 3B). Viral titers of supernatants from WNV-inoculated cells were also measured by plaque assay. Consistently, this demonstrated that viral titers of supernatants from WNV-inoculated cells were significantly decreased in a dose-dependent manner in the presence of either EerI or MDBN (Fig. 3C). The inhibitory effects of EerI in WNV infection were confirmed in a different cell line, human neuroblastoma SK-N-SH cells. Inhibition of VCP by EerI both decreased the percentage of WNV-infected cells and viral titer in SK-N-SH cells (Fig. 4). These findings suggest that VCP may play a role in WNV infection.

Fig. 2

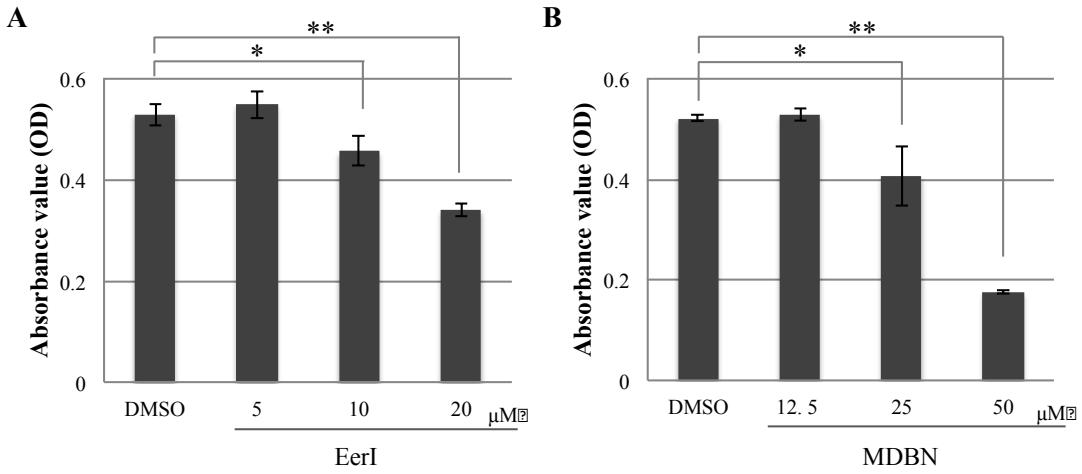

Cell viability of HeLa cells after treatment with either EerI or MDBN

The HeLa cells were treated with the indicated concentrations of either EerI (A) or MDBN (B). Cell viability was examined by a MTT assay at 24 h post treatment. * $p < 0.05$, ** $p < 0.01$ (one-way ANOVA).

Fig. 3

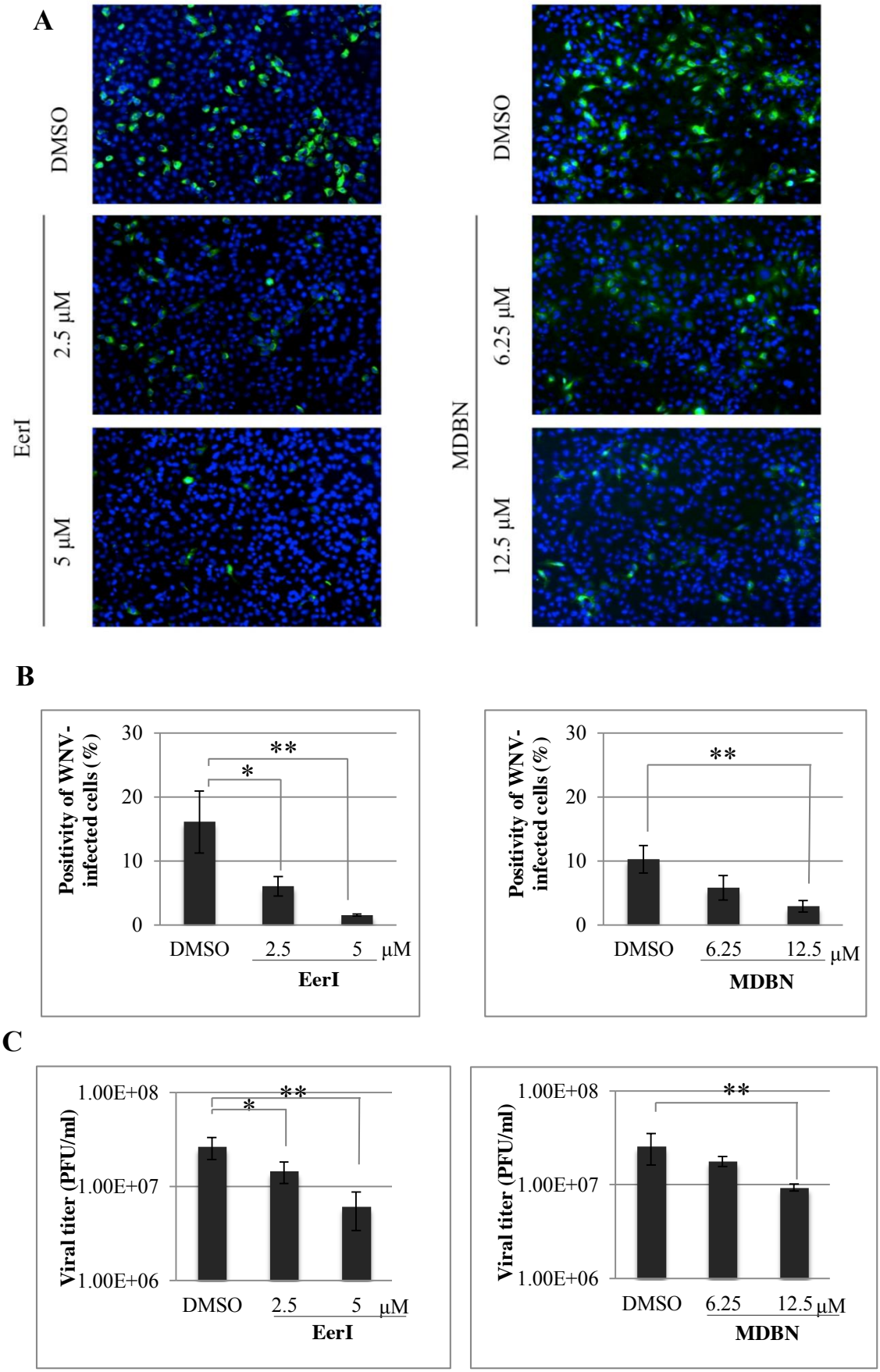
A
DMSO
EerI
2.5 μM
5 μM
MDBN
6.25 μM
12.5 μM
B
Positivity of WNV-infected cells (%)
30
20
10
0
**
*
DMSO
2.5
5
μM
EerI
Positivity of WNV-infected cells (%)
**
DMSO
6.25
12.5
μM
MDBN
C
Viral titer (PFU/ml)
1.00E+08
1.00E+07
1.00E+06
**
*
DMSO
2.5
5
μM
EerI
Viral titer (PFU/ml)
1.00E+08
1.00E+07
1.00E+06
**
DMSO
6.25
12.5
μM
MDBN

WNV infection is inhibited in the presence of VCP inhibitors.

(A) WNV infection in the presence of either EerI (left panels) or MDBN (right panels). HeLa cells were inoculated with WNV (MOI=1) and then treated with EerI or MDBN at 1 hpi Cells were harvested at 24 hpi and stained with anti-JEV antibody (Kimura et al., 1994; Kobayashi et al., 2012) that has cross reactivity with WNV antigen (green). Cell nuclei were counterstained with DAPI (blue). (B) Positivity of WNV-infected cells from (A). Mean ± SD from triplicate experiments is shown; * $p < 0.05$, ** $p < 0.01$ (one-way ANOVA). (C) The culture supernatants from (A) were collected at 24 hpi and the viral titers of the harvested supernatants were examined by plaque assay. Mean ± SD from three independent experiments is shown; * $p < 0.05$, ** $p < 0.01$ (one-way ANOVA).

Fig. 4

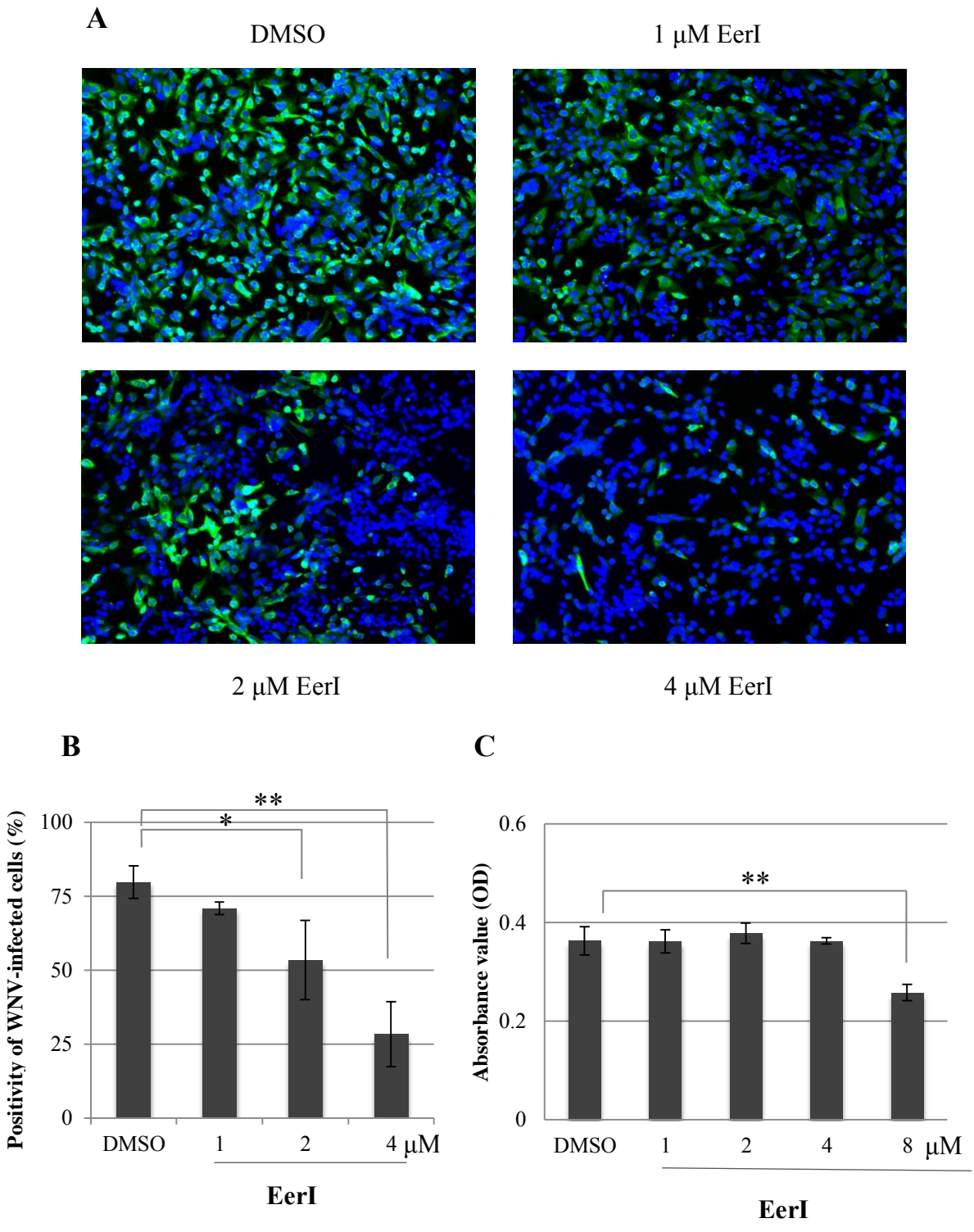
A
DMSO
1 μM EerI
2 μM EerI
4 μM EerI
B
Positivity of WNV-infected cells (%)
100
75
50
25
0
**
*
DMSO
1
2
4 μM
EerI
C
Absorbance value (OD)
0.6
0.4
0.2
0
**
DMSO
1
2
4
8 μM
EerI

WNV infection in SK-N-SH cells is attenuated in the presence of EerI.

(A) WNV infection in human neuroblastoma, SK-N-SH cells. SK-N-SH cells were inoculated with WNV (MOI=1). After 1 hpi, the inoculated-cells were treated with EerI at the indicated concentration. DMSO treated-cells were used as control. The cells were fixed and prepared for IFA at 24 hpi and stained with anti-JEV antibody, which has cross reactivity with WNV antigen (green). Cell nuclei were stained with DAPI (blue). (B) Positivity of WNV-infected cells from (A). Mean ± SD from triplicate experiments is shown; * $p < 0.05$. ** $p < 0.01$ (one-way ANOVA). (C) Cell viability of SK-N-SH at 24 h after exposure to EerI with absorbance values obtained after MTT assay.

WNV infection is inhibited by knockdown of VCP

To confirm that the inhibition of WNV infection was caused by perturbation of VCP activity, siRNAs were employed to deplete endogenous VCP. HeLa cells were transfected with either of three siRNAs targeting three different regions of the VCP gene [siVCP (1), (2) and (3)] or a control siRNA (siCont) and then inoculated with WNV 48 h post transfection and incubated for 24 h. The expression level of VCP after silencing was confirmed by immunoblotting. Reverse transfection of siVCP (1) and (3) for 48 h strongly decreased expression levels of endogenous VCP in HeLa cells (Fig. 5A). Furthermore, depletion of endogenous VCP reduced expression levels of WNV-E protein at 24 hpi of WNV (Fig. 5A). And, siRNA targeting of VCP [(1) and (3)] significantly reduced the percentage of WNV-infected cells (Fig. 5B and 5C). However, siRNA (2) failed to knockdown endogenous VCP as shown in the immunoblotting and IFA results (Fig. 5A, 5B and 5C). The viral titers in supernatants of WNV-inoculated HeLa cells treated by the siRNAs against VCP were further measured. Plaque assays revealed that the viral release was significantly inhibited by siRNA treatment [siCVP (1) and (3)] (Fig. 5D). The effect of siRNA against VCP on WNV infection by IFA at different time points (12, 24 and 48 h) was examined. A decrease in the immunofluorescence signals between cells transfected with control and VCP siRNAs was detected (Fig. 6). These results indicate that a depletion of VCP significantly inhibits WNV infection. In contrast, VCP-knockdown did not affect infection by recombinant-VSV (Fig. 7).

Fig. 5

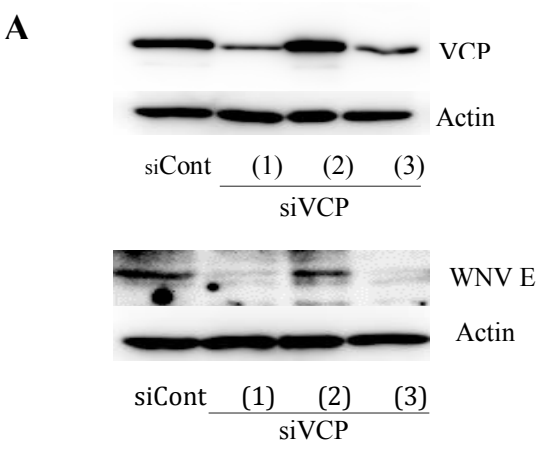
A
VCP
Actin
siCont (1) (2) (3)
siVCP
WNV E
Actin
siCont (1) (2) (3)
siVCP

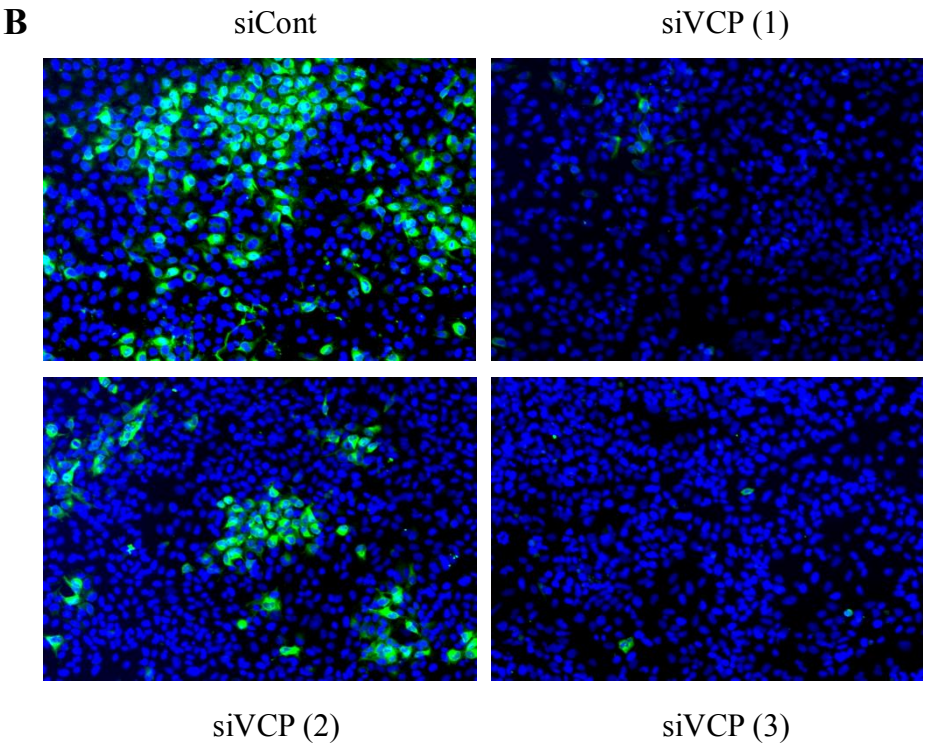
B
siCont
siVCP (1)
siVCP (2)
siVCP (3)

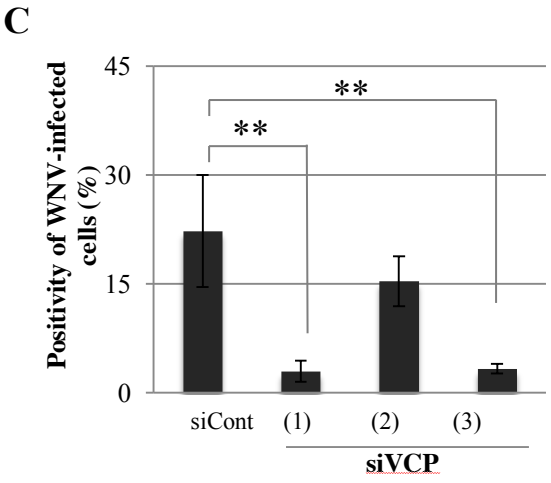
C
Positivity of WNV-infected cells (%)
45
30
15
0
**
**
siCont (1) (2) (3)
siVCP

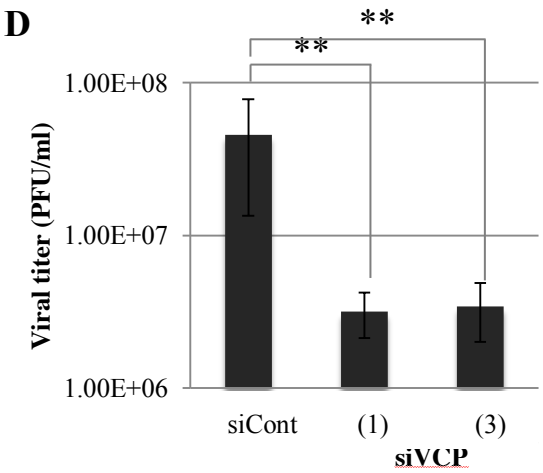
D
Viral titer (PFU/ml)
1.00E+08
1.00E+07
1.00E+06
**
**
siCont (1) (3)
siVCP

WNV infection is inhibited in VCP knockdown cells.

(A) HeLa cells were treated with either siRNA against VCP [siVCP (1), (2) and (3)] or control siRNA (siCont). The siRNA-treated cells were inoculated with WNV (MOI=1) at 48 hpi. The inoculated cells were harvested at 24 hpi. The expression of endogenous VCP protein and WNV envelope protein after treatment with the indicated siRNA were examined by immunoblotting with mouse anti-VCP antibody and mouse anti-WNV/Kunjin envelope protein. The expression of actin was examined after reprobing as an endogenous control. (B) WNV-infected cells from (A), after 24 h incubation with WNV, the cells were harvested and examined by IFA. WNV-infected cells were stained with anti-JEV antibody (green) and cell nuclei were counterstained with DAPI (blue). (C) Positivity of WNV-infected cells from (B). Mean ± SD from three independent experiments is shown; ** $p < 0.01$ (one-way ANOVA). (D) The culture supernatants from (A) were collected at 24 hpi and the viral titers of the harvested supernatants were determined using plaque assay. Mean ± SD from three independent experiments is shown; ** $p < 0.01$ (one-way ANOVA).

Fig. 6

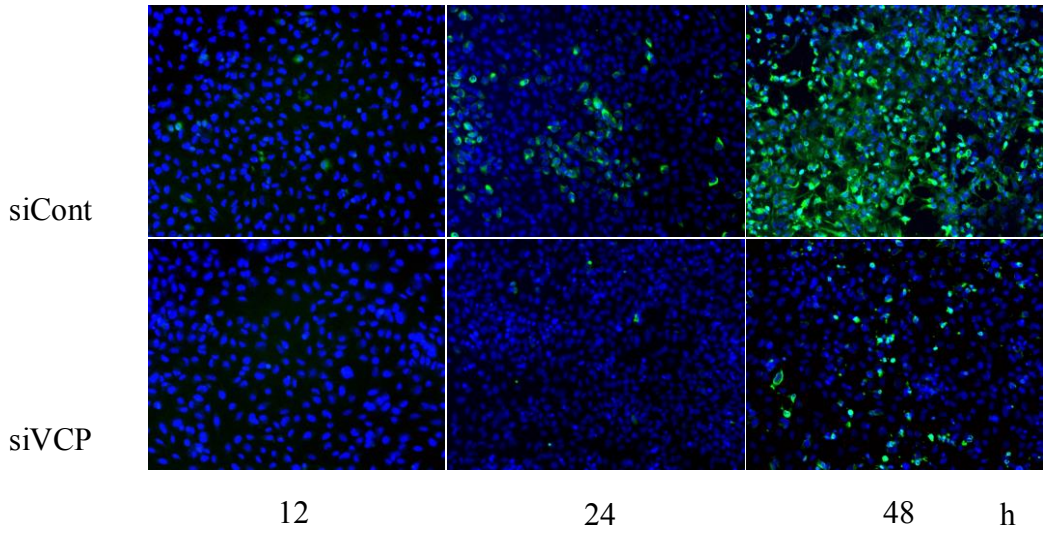

Representative figure showing IFA results of WNV infection in siVCP compared to siCont treated-HeLa cells at 12, 24 and 48 hpi

The HeLa cells were treated with either siVCP or siCont and then incubated at 37 °C for 48 h. Thereafter, the cells were infected with WNV (MOI=1) and incubated at 37 °C for 12, 24 and 48 hpi, respectively. After incubation at the indicated time points, the cells were then fixed and prepared for IFA followed by staining with anti-JEV antibody that has cross reactivity with WNV antigen (green). Cell nuclei were stained with DAPI (blue).

Fig. 7

A

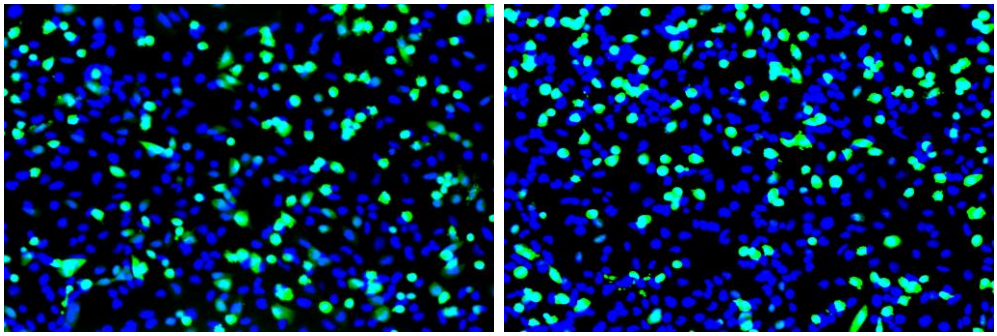

B

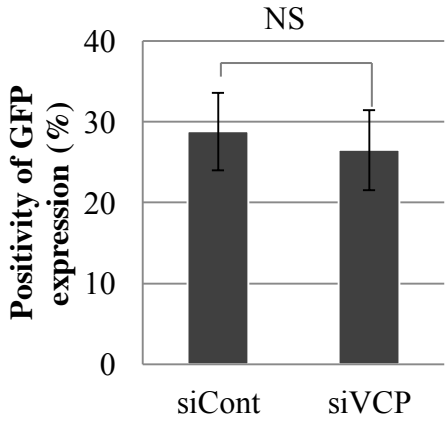

VCP knockdown does not affect infection of recombinant-VSV.

(A) HeLa cells were treated with siRNA against VCP (siVCP) or control siRNA (siCont) for 48 h. Thereafter, the siRNA-treated cells were inoculated with recombinant-VSV. Recombinant-VSV positive cells were determined by expression of GFP, which was carried by the recombinant-VSV replicon, at 8 hpi nuclei were stained with DAPI (blue). (B) The positivity of GFP from (A). Mean ± SD from triplicate experiments is shown. The significance was analyzed using a one-way ANOVA.

VCP participates in the early and genome replication steps during the WNV life cycle

Next, the specific role of VCP in the life cycle of WNV was investigated. The intracellular life cycle of WNV is divided into two major steps, early and late (Fernandez-Garcia et al., 2011; Kaufmann and Rossmann, 2011). The early step consists of viral attachment, entry and uncoating (Jiang et al., 2010; Kaufmann and Rossmann, 2011), while the late step involves genome translation, genome replication, viral assembly and release (Kobayashi et al., 2016). WNV-VLPs were employed to determine whether VCP participates in the early or late replication steps (Kobayashi et al., 2014). WNV-VLPs are unable to produce progeny virions because of the absence of WNV structural protein-coding sequences in their genome. Therefore, the results are independent of the assembly and virion-releasing steps (Hasebe et al., 2010; Scholle et al., 2004). Thus, WNV- VLPs allow the determination of whether VCP plays a role in either an early step or during the genomic replication of the WNV life cycle. WNV-VLPs were inoculated into both VCP and control siRNA-transfected cells and monitored by expression of DsRed-encoded in the WNV-VLP replicon. qRT-PCR demonstrated that the quantity of WNV-RNA in VCP-knockdown cells was significantly lower than that in control siRNA-treated cells (Fig. 8A). These results suggest that VCP-knockdown significantly inhibits infection of WNV-VLPs through an inhibition of early step and/or genome replication steps of the WNV life cycle.

To confirm the role of VCP in the early stages of WNV replication, the siRNA-treated cells were inoculated with WNV and the viral RNA was investigated at an early time point of WNV infection, at 2 h post infection. The result revealed that silencing of VCP significantly decreased the quantity of WNV-RNA at 2 h post

inoculation of WNV compared to control siRNA treated-cells (Fig. 8B). This suggests that VCP plays a role in the early step of WNV replication cycle, including attachment or entry into cells.

To examine whether VCP plays a role in the late step of the WNV life cycle, three plasmids encoding WNV sequences (pCMV-C, pCMV-SVP and pCMV-WNrep-DsRed) were co-transfected into either VCP-knockdown or control siRNA-treated cells. The plasmid transfection protocol for VLP production has been previously employed to investigate the role of host factor(s) in the late stages of viral infection, including genome replication and virus release (Kobayashi et al., 2016). The components of the VLP are transfected into cells, therefore, the results obtained employing the plasmid-encoded VLPs were not associated with the early steps of WNV replication (Kobayashi et al., 2016). At 72 h after plasmid transfection, the WNV-VLP titers in the supernatants from plasmid transfected-cells were examined. The titer of WNV-VLPs was significantly decreased in VCP-knockdown [siVCP (1)] cells compared with control siRNA-treated cells (Fig. 8C). These data suggest that VCP is also involved in the genome replication and/or assembly and release steps of the WNV life cycle.

To confirm that VCP is important for WNV genome replication, the WNV DNA-based replicon pCMV-WNrep-DsRed was introduced into both VCP knockdown and control siRNA-treated cells. This replicon consists of coding sequences of WNV non-structural proteins, while almost all of the sequences encoding WNV structural proteins were deleted and replaced by sequences encoding DsRed. The replicon can replicate and translate to synthesize viral genomic RNA and the non-structural proteins of WNV, respectively. However, it is not capable of producing viral progeny because of the absence of structural protein sequences of

WNV. The results of qRT-PCR of the plasmid-transfected cells at 72 h post transfection demonstrated a 10-fold reduction of synthesized WNV-RNA in the VCP-knockdown cells compared to control siRNA-treated cells (Fig. 8D). Taken together, these data indicate that VCP plays a role in the genome replication of the WNV life cycle.

Fig. 8

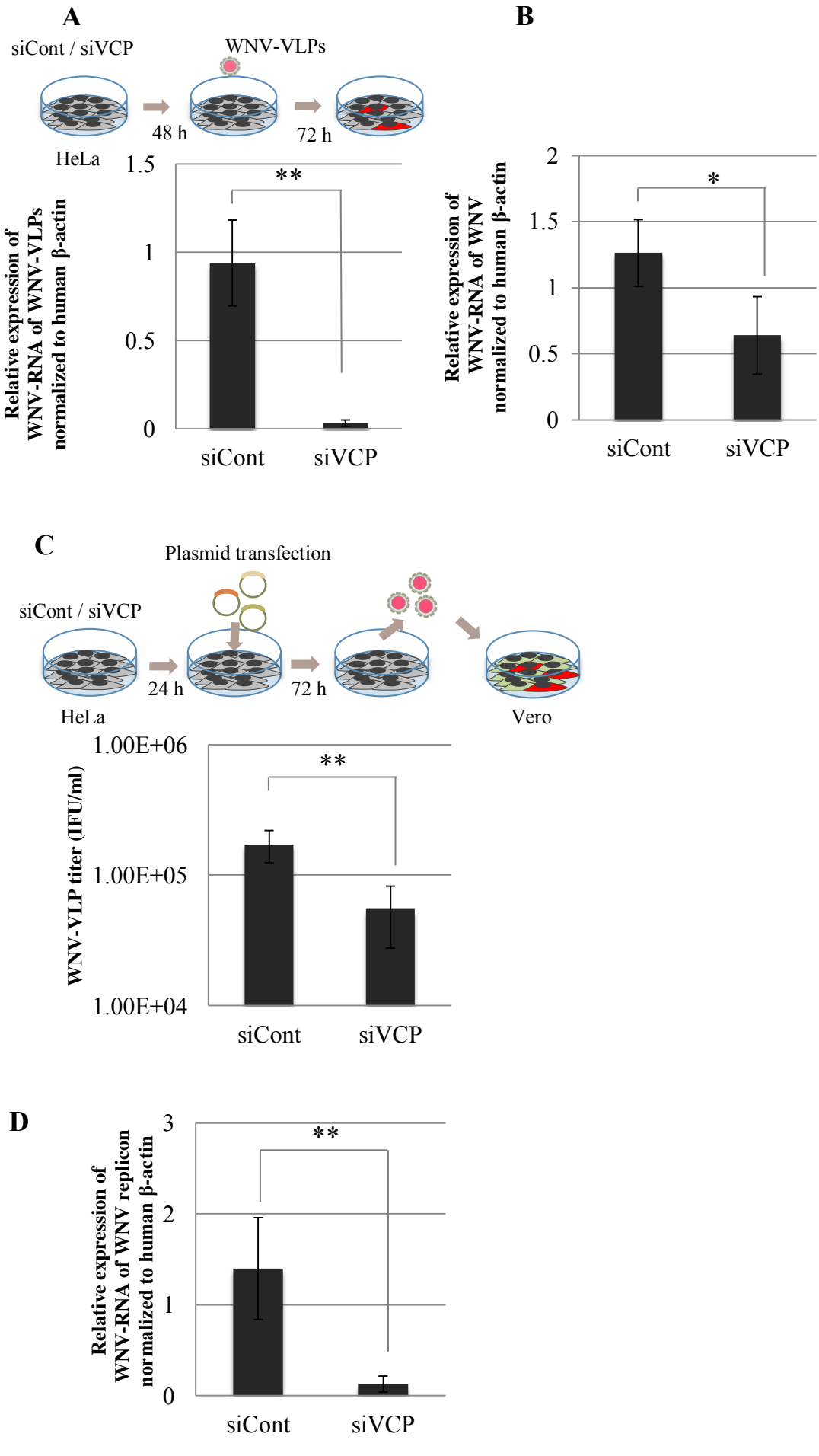
A
siCont / siVCP
WNV-VLPs
48 h
72 h
HeLa
Relative expression of WNV-RNA of WNV-VLPs normalized to human β-actin
1.5
1
0.5
0
**
siCont
siVCP
B
Relative expression of WNV-RNA of WNV normalized to human β-actin
2
1.5
1
0.5
0
*
siCont
siVCP
C
Plasmid transfection
siCont / siVCP
24 h
72 h
HeLa
Vero
WNV-VLP titer (IFU/ml)
1.00E+06
1.00E+05
1.00E+04
**
siCont
siVCP
D
Relative expression of WNV-RNA of WNV replicon normalized to human β-actin
3
2
1
0
**
siCont
siVCP

The role of VCP in distinct steps of WNV life cycle was investigated.

(A) WNV-VLP infection after the indicated siRNA treatment, HeLa cells were treated with siRNA against VCP, siVCP (1) or control siRNA (siCont). The indicated siRNA treated-cells were inoculated with WNV-VLPs (16 HAU) at 48 h post transfection and incubated for 72 h. Relative quantification of WNV-RNA normalized to human β-actin from (A) examined by qRT-PCR. Mean ± SD from three independent experiments is shown; ** $p < 0.01$ (one-way ANOVA). (B) Relative quantification of WNV-RNA expression levels normalized to human β-actin of siRNA-treated cells inoculated with WNV at the early time point of infection. siRNA-treated HeLa cells were inoculated with WNV after 48 h post siRNA transfection. The inoculated cells were incubated on ice for 1 h, followed by washing 5 times with PBS and then transferred to 37 °C. After 1 h incubation, the cells were harvested by trypsin and prepared for qRT-PCR. Mean ± SD from two independent experiments in triplicate is shown; * $p < 0.05$ (one-way ANOVA). (C) HeLa cells were treated with siRNA against VCP, siVCP (1) or control siRNA (siCont). After 24 h post transfection, the cells were transfected with plasmid set for WNV-VLP production and incubated for 72 h. The culture supernatants were harvested and inoculated on Vero cell monolayers in 10-fold serial dilutions. The viral titers of the harvested supernatants were determined as IFU/ml. Mean ± SD from three independent experiments is shown; ** $p < 0.01$ (one-way ANOVA). (D) HeLa cells were treated with siRNA, either siVCP (1) or siCont, and then transfected with plasmid containing WNV DNA replicon, pCMV-WNrep-DsRed at 24 h post siRNA treatment and incubated. The transfected cells were harvested at 72 h post transfection of pCMV-WNrep-DsRed. Relative quantification of WNV-

RNA normalized to expression of human β-actin was examined by qRT-PCR. Mean ± SD from three independent experiments is shown; ** $p < 0.01$ (one-way ANOVA).

Discussion

In the present study, the roles of VCP during WNV infection was investigated. The perturbation of endogenous VCP using a potent VCP inhibitor or siRNA targeting VCP significantly inhibited WNV infection. The expression of endogenous VCP in HeLa cells is depleted after 48 h siRNA transfection [with siVCP (1) and (3)] was confirmed, while another siRNA siVCP (2) did not silence expression of endogenous VCP. Silencing of endogenous VCP, by siVCP (1) and (3), demonstrated that depletion of VCP significantly suppressed WNV infection. This finding suggests that VCP is required for WNV infection. Thereafter, the most potent siRNA [siVCP (1)] was employed to investigate the roles of VCP in WNV replication. A previous report indicated that silencing of endogenous VCP and nuclear protein localization 4 (NPL4), a VCP cofactor, did not inhibit WNV infection, whereas depletion of ubiquitin fusion degradation 1-like (UFD1L) and p47, other cofactors of VCP, suppressed WNV infection (Krishnan et al., 2008). It is suggested the differences between this previous report and the present results may be related to the use of different strains of WNV or could be related to the silencing efficiency of the siRNA employed in the experiments. In addition, control experiments from the present study using recombinant-VSV demonstrated that depletion of VCP did not suppress recombinant-VSV infection. These results suggest that VCP plays a role in WNV infection specifically and inhibition of WNV infection in VCP knockdown cells is not a consequence of cellular cytotoxicity.

Employing VLPs, perturbation of VCP suppressed the infectivity of WNV-VLPs was demonstrated (Fig. 8A). This indicates that VCP is potentially involved in either the early steps or during genome replication of WNV. Using plasmid

transfection to generate WNV-VLPs, bypassing the early steps of the WNV life cycle, the role of VCP in the late steps (from genome replication until virus release) of the viral life cycle was examined. Knockdown of VCP reduced the yield of WNV-VLPs compared to control siRNA-treated cells (Fig. 8C) and this finding suggests that VCP also participates in the late steps of WNV life cycle. Taken together, it is hypothesized that VCP may be implicated in the genome replication steps of WNV. Therefore, a WNV DNA-based replicon was employed to clarify whether VCP is required for genome replication of WNV. Depletion of VCP significantly decreased expression levels of synthesized WNV-RNA (Fig. 8D) and this finding indicates that VCP is engaged in WNV genomic RNA replication.

It has been previously reported that VCP was found to be localized in the cytosol, ER and nucleus, and can play a role in several cellular processes (Arita et al., 2012; Meyer et al., 2012; Meyer and Weihl, 2014; Yamanaka et al., 2012). The possible mechanism(s) of VCP involvement in WNV infection may be based on the localization and physiological function of VCP. Functional roles of VCP in the replication of the WNV-related flaviviridae virus, hepatitis C virus (HCV) have been reported (Yi et al., 2016). VCP knockdown significantly decreased expression of HCV RNA levels and VCP was found to be colocalized with the HCV replication complex. It is thus possible that this function of VCP in the HCV life cycle is also required for WNV genome replication, however, no direct evidence currently exists for an interaction between WNV replicase components and VCP and further investigations are required.

Apart from during the genome replication of the WNV life cycle, VCP might potentially be involved in other steps. The present study demonstrates that VCP may also function in the early steps, during either attachment or entry, of the viral life

cycle (Fig. 8B). The results of an entry assay revealed that silencing of endogenous VCP caused a significant reduction in the expression levels of WNV-RNA compared to control siRNA-treated cells. This suggests that VCP may also play a role in either the binding or entry steps of the WNV life cycle. A role for VCP in early stages of viral infection has previously been reported for coronavirus and Sindbis virus (Panda et al., 2013; Wong et al., 2015). Depletion of VCP inhibited coronavirus infection through a failure in the maturation of virus-loaded endosomes leading to accumulation of coronavirus particles in the early endosomal compartment (Wong et al., 2015). Studies on Sindbis virus indicated that VCP functioned as a regulator of viral entry as knockdown of VCP caused an alteration of trafficking and resulted in the degradation of Sindbis virus entry receptor (Panda et al., 2013). However, the possible function of VCP on early stages of WNV replication has not been investigated and will require further study.

In conclusion, these findings suggest that VCP is required for replication of WNV at a number of different stages of the viral life cycle, thus, VCP potentially represents a candidate for the therapeutic inhibition of WNV infection.

Summary

The present study demonstrates the role of VCP in WNV infection. WNV infection is significantly inhibited by perturbation of VCP either chemical inhibitors or siRNA targeting to VCP. According to the present data using WNV-VLPs and WNV-DNA-based replicon, VCP is engaged in both early and genome replication steps of WNV replication cycle. However, the precise mechanism of role of VCP in WNV infection has not been investigated yet and further study might be required. It is suggested that VCP might be a promised target for development of therapeutic medicine of WNV infection.

Chapter II

An examination of the pathogenicity of novel WNV strain isolated in Zambia

Introduction

WNV was firstly isolated in Uganda in 1937 as previously described. WNV has been spread through many continents, including Africa, Asia, Middle East, Europe, Australia and America with existing of five lineages based on genetic classification (Bondre et al., 2007). However, most of identified strains mainly belong to the lineage 1 and 2, which cause the disease in human and other vertebrates. The lineage 1 has been identified in North America, North Africa, Europe and Australia. Whereas, lineage 2 has been mostly detected in Africa, Madagascar and has been introduced to Central, Eastern and Southern Europe recently (Hernández-Triana et al., 2014; Magurano et al., 2012; Venter and Swanepoel, 2010). Lineage 3 and 4 were detected in Europe; however it has not been reported that these two lineages naturally cause disease in vertebrate. Lineage 5 was isolated from the human patient in India (Bondre et al., 2007).

The lineage 2 has been responsible for endemic in Africa (Venter and Swanepoel, 2010). The virus has been endemic since the 1950's and *Culex univittatus* has been reported as a main vector for WNV in Africa. The major outbreak of WNV in Africa occurred in South Africa in 1970 and the virus has been maintained through enzootic cycle between avian species and *Culex univittatus (C. univittatus)*. The republic of Zambia is located in southern part of Africa. A cross-sectional study of seroprevalence of WNV IgG and IgM antibodies revealed that 10.3% of the

population in North Western and Western provinces of Zambia had been infected with WNV (Mweene-Ndumba et al., 2015). However, the WNV has not been isolated yet. The member of my current laboratory could detect and isolate the novel strain of WNV in mosquito sample, *C. quinquefasciatus*, collected from western part of Zambia in 2016 (Orba et al., in submission) (Fig. 9). The study demonstrated that the Zambian isolate was genetically close to South African strains in the lineage 2 (Fig. 10) which have been reported to be neuroinvasive. However, the pathogenicity of the Zambian isolate has not been evaluated yet. In this study, mortality rate, body weight loss and viral load in the brain of Zambian isolate-inoculated mice was compared with those of either high-pathogenic NY99 6-LP strain or low-pathogenic Eg101 strain.

Fig. 9

Location of sampling area, Mongu province in Western Zambia and Lusaka, capital city of Zambia.

Fig. 10

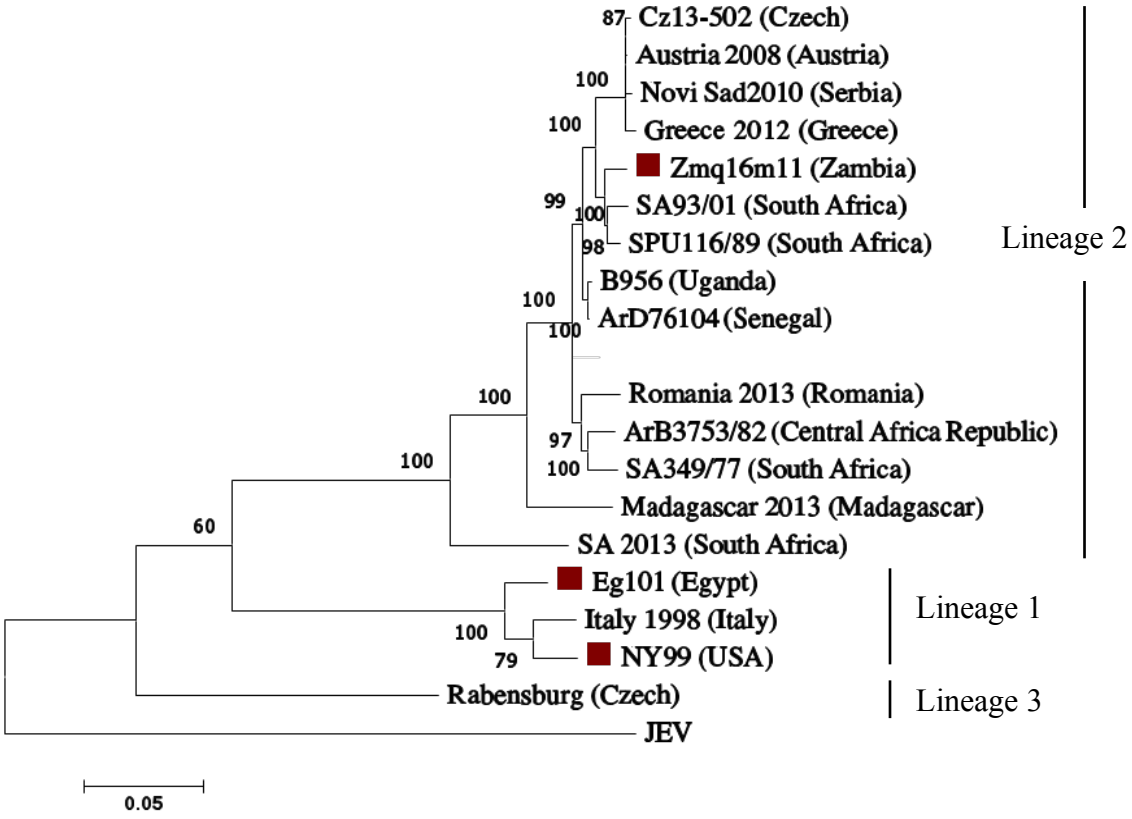

The molecular phylogenetic analysis of full length of WNV genome sequences

Sequences of WNV strains obtained from GenBank were aligned with ClustalW, and phylogenetic analysis was performed by using Maximum Likelihood methods based on the Jukes-Cantor model with 1,000 bootstrap replicates using MEGA7 software. GenBank accession no. are as follows: Cz13-502 (KM203863), Austria 2008 (KF179640), Novi Sad2010 (KC496016), Greece 2012 (KF179639), SA93/01 (EF429198), SPU116/89 (EF429197), B956 (AY532665), Ard76104 (DQ318019), Romania 2013 (KJ934710), ArB3753/82 (DQ318020.1), AS349/77 (KM052152), Madagascar 2013 (HM147823), SA 2013 (HM147822), Eg101 (AF260968), Italy 1998 (AF404757), NY99 (DQ211652), Rabensburg (AY765264) and JEV (AY303791).

Materials and Methods

Viruses

Three strains of WNV, including Zambian isolate, NY99 6-LP and Eg101 strain were propagated in mosquito C6/36 cells and the viral titers were measured by plaque assay as previously described in the chapter I.

Animals and experimental infection

C57BL/6JCr Slc mice (6 week-old female) were used in this experiment. All animal experiments were performed at the BSL-3 facility in accordance with institutional guidelines, and ethical permission was obtained from the Hokkaido University Animal Care and Use Committee. Each WNV strain was inoculated to mouse by either intraperitoneal (IP, 100 PFU) or intracranial (IC, 1 PFU) injection. To minimize the pain, each mouse was anesthetized by isoflurane inhalation before viral inoculation. The body weight and mortality were observed every day until 15 days post inoculation (dpi). The median survival time is defined as the time point when the 50% of mice have died. The mouse experiments were performed twice at different time. Therefore, the experiment needs to be repeated to confirm the obtained results.

Tissue and blood collection

The tissue and blood samples of WNV-infected mice were collected with aseptic technique at 6 and 9 dpi after deep anesthesia by isoflurane inhalation. After collection of the whole blood, the blood was separated as clot and serum by leaving it at room temperature for 15 mins. The clot was removed by centrifugation at 2,000 x *g*

for 10 minutes at 4 °C. Clear straw-colored serum was collected and stored at -80 °C until use.

Serum, spleen and brain samples of each WNV-inoculated mouse were collected for plaque assay, RNA isolation and immunohistopathological examination for future experiments. Tissue samples for plaque assay and RNA isolation were put into 1.5 microcentrifuge tubes and stored at -80 °C until use.

Plaque assay

Plaque assay was employed to measure viral titers in tissue samples collected from WNV-infected mice. The tissue samples were homogenized and prepared as 10% homogenates with PBS. The tissue homogenates and serum samples were diluted with PBS in series of 10-fold dilutions. Each diluted sample (200 µl) was applied onto monolayer of Vero cells grown in 12-well plates. The cells were grown in MEM containing 5% FBS, 2 mM of L-glutamine and 1.25% methycellulose, at 37 °C for 4 days or until the plaque was able to clearly recognized.

Results

1. Survival rates, body weight change and viral titers in brain after IP inoculation of WNV

The survival rate of mice inoculated with either Zambian isolate, NY99 6-LP or Eg101 strain by IP method (100 PFU/mouse) was compared. The survival rates of mice at 15 dpi after inoculation with Zambian isolate, NY99 6-LP and Eg101 by IP method, were 5% (n=20), 25% (n=20) and 40% (n=20), respectively (Fig. 11).

Next, body weight change after IP inoculation with each WNV strain was examined (Fig. 12). The WNV inoculated mice showed clinical symptoms such as weight loss, ruffled fur, swollen eyes and neurological sign (hind limbs paralysis etc.). Ten and twenty percent of body weight decrease seems to be related to morbidity and mortality of the WNV-inoculated mice, respectively (Fig. 12). In some mice inoculated with Zambian isolate by IP method, body weight loss was observed, suggesting that Zambian isolate had virulence to the inbred mice.

After IP inoculation with each WNV strain, serum, spleen and brain were harvested at 6 and 9 dpi for measurement of the viral titers. The viral titers of serum samples both from 6 dpi and 9 dpi were below the limit of detection by a plaque assay method (data not shown). The viral titers were detected in spleen of mice inoculated with Zambian isolate, NY99 6-LP and Eg101 at 6 dpi. There was no statistic difference in viral titers in the spleen among the three strains (data not shown). Whereas, the viral titers of all spleen tissues collected from 9 dpi were below the limit of detection.

The average of viral titers detected in brain tissue of mice inoculated by IP method with Zambian isolate, NY99 6-LP and Eg101, were 22, 367 and 285 at 6 dpi,

and 3.5, 852 and 917 PFU/mg at 9 dpi, respectively (Fig. 13).

Viral titers of brain from Zambian isolate-inoculated mice by IP method were detected, suggesting that Zambian isolate had reached to the brain tissue after peripheral IP inoculation method. According to the obtained results, the titers of brain from Zambian isolate-inoculated mice were much lower than those of NY99 6-LP- and Eg101-inoculated mice at 6 and 9 dpi.

IP inoculation of Zambian isolate caused higher mortality than high-pathogenic NY99 6-LP and low-pathogenic strain Eg101 strains. However, the viral titers of brain from Zambian isolate-inoculated mice by IP method were much lower than those of brains from NY99 6-LP- and Eg101-inoculated mice. These results suggest that Zambian isolate may have low ability to pass through the blood brain barrier (BBB) and/or to replicate in brain. In addition, Zambian isolate may promote high production of cytokines related to innate immune response, resulting in tissue injury. Next, to examine the mortality of inoculation with each WNV strain after step of passing the BBB, IC inoculation method was applied.

Fig. 11

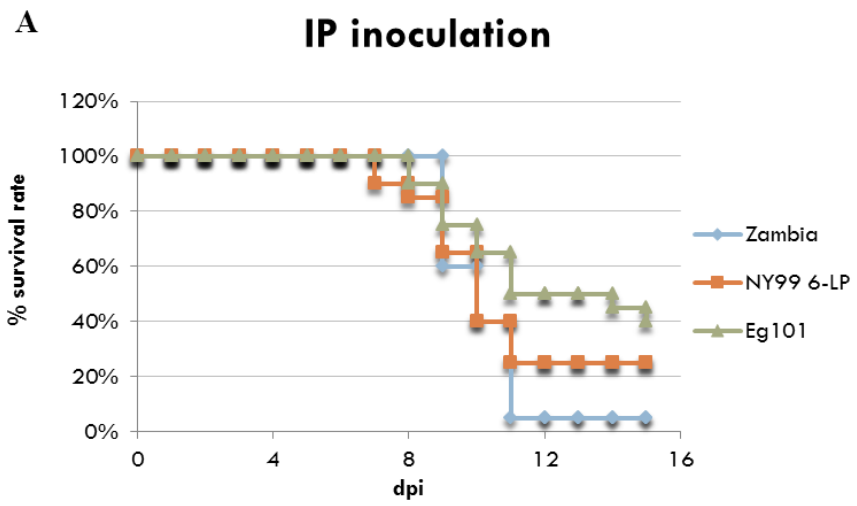

The survival rate after inoculation with each strain of WNV

Mice were inoculated with each WNV strain by IP (100 PFU; A) or IC (1 PFU; B) method. The mice were observed mortality and body weight for 15 days.

Fig. 12

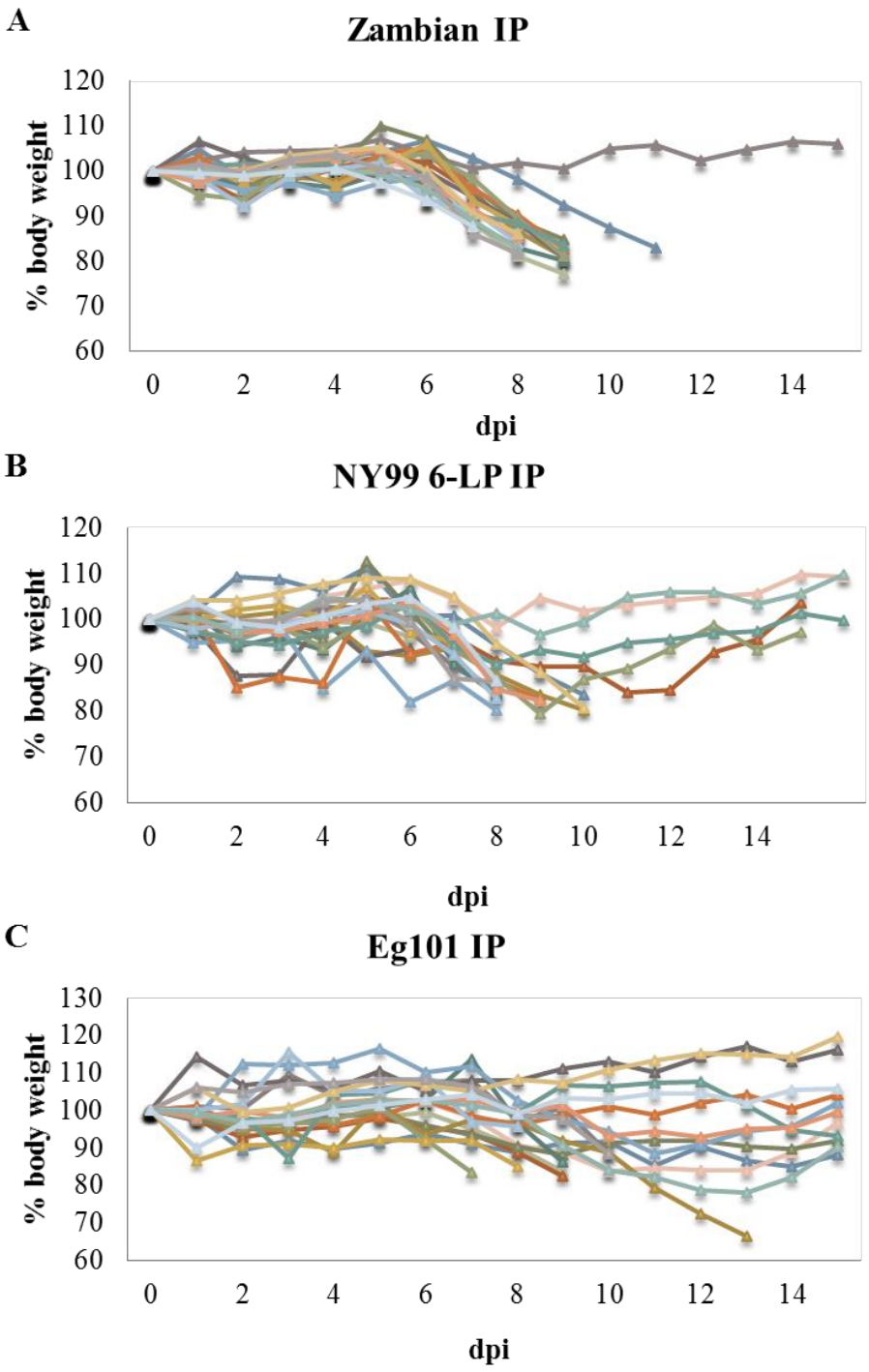

The body weight change of each mouse inoculated with WNV strain by IP method

Each WNV strain, including Zambian isolate (A), NY99 6-LP strain (B) or Eg101 strain (C) (100 PFU/mouse) was inoculated with IP method.

Fig. 13

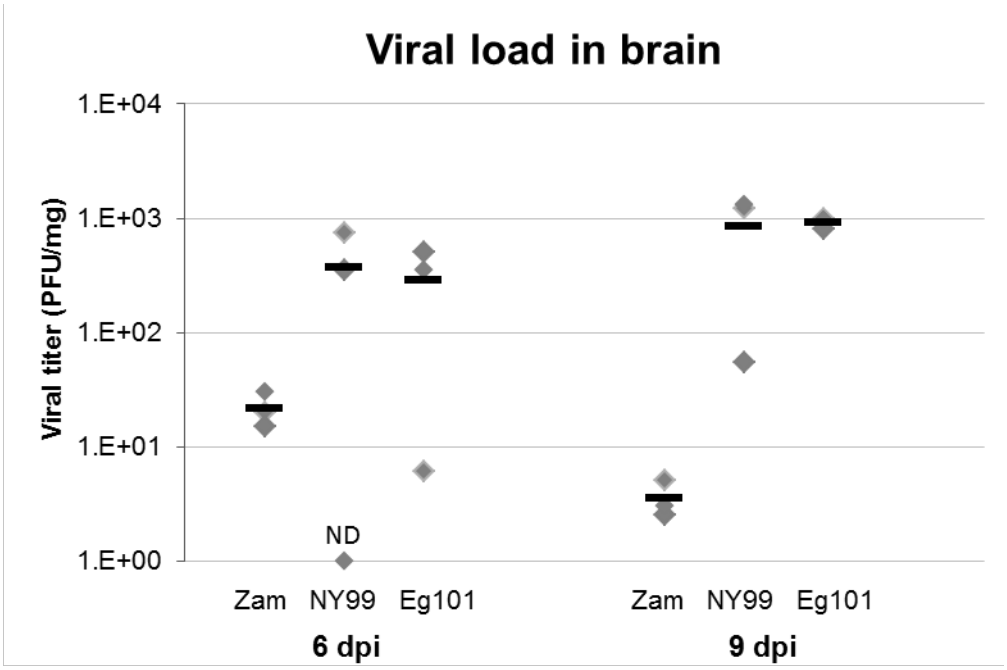

The viral titers in brain tissue of mice inoculated with each WNV strain by IP method

The brain samples were collected at 6 and 9 dpi (n=3). The samples were prepared as 10% homogenates with PBS. The viral titers of homogenates were measured by a plaque assay.

2. Survival rates and body weight change after IC inoculation of WNV

Next, the survival rate of mice inoculated with either Zambian isolate, NY99 6-LP or Eg101 strain by IC method (1 PFU/mouse) was compared. The survival rates of mice at 15 dpi after IC inoculation with Zambian isolate, NY99 6-LP and Eg101 were 35% (n=20), 5% (n=19) and 26% (n=19), respectively (Fig. 14). Some of WNV-inoculated mice had body weight loss around 4 dpi with clinical symptoms (Fig. 15).

The median survival time (MST) of inoculation of Zambian isolate either by IP or IC injection was 10 dpi (Table 1). Meanwhile, the MST of mice after inoculation with either NY99 or Eg101 strain through IP injection were 10 and 11 dpi, respectively. And, the MST after inoculation of NY99 or Eg101 with IC method was 8 dpi (Table 1). These results suggest that Zambian isolate may have less neuronal injury activity than NY99 6-LP and Eg101 strains. However, as described in the Materials and Methods section, these WNV-inoculation experiments were performed only two times, therefore these experiments needs to be repeated to confirm obtained results.

Fig. 14

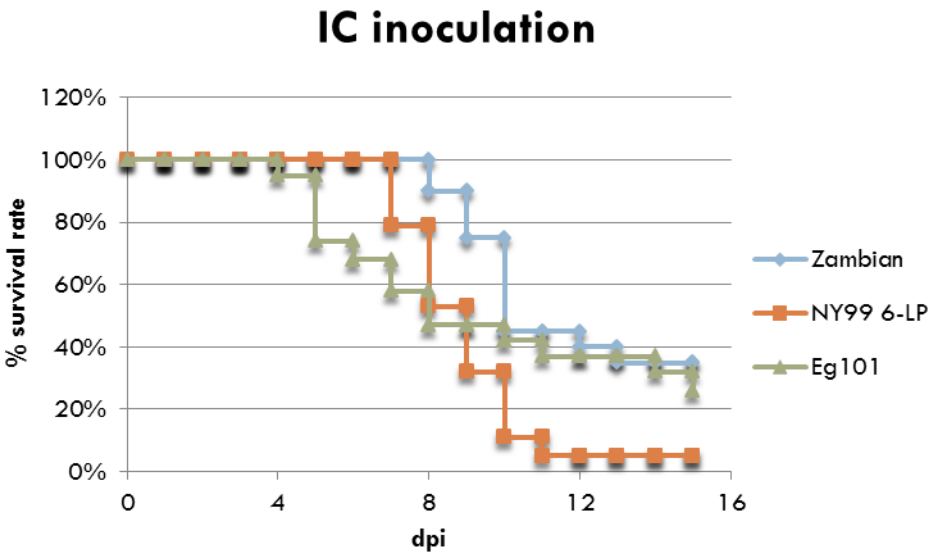

The survival rate after inoculation with each strain of WNV

Mice were inoculated with each WNV strain by IP (100 PFU; A) or IC (1 PFU; B) method. The mice were observed mortality and body weight for 15 days.

Fig. 15

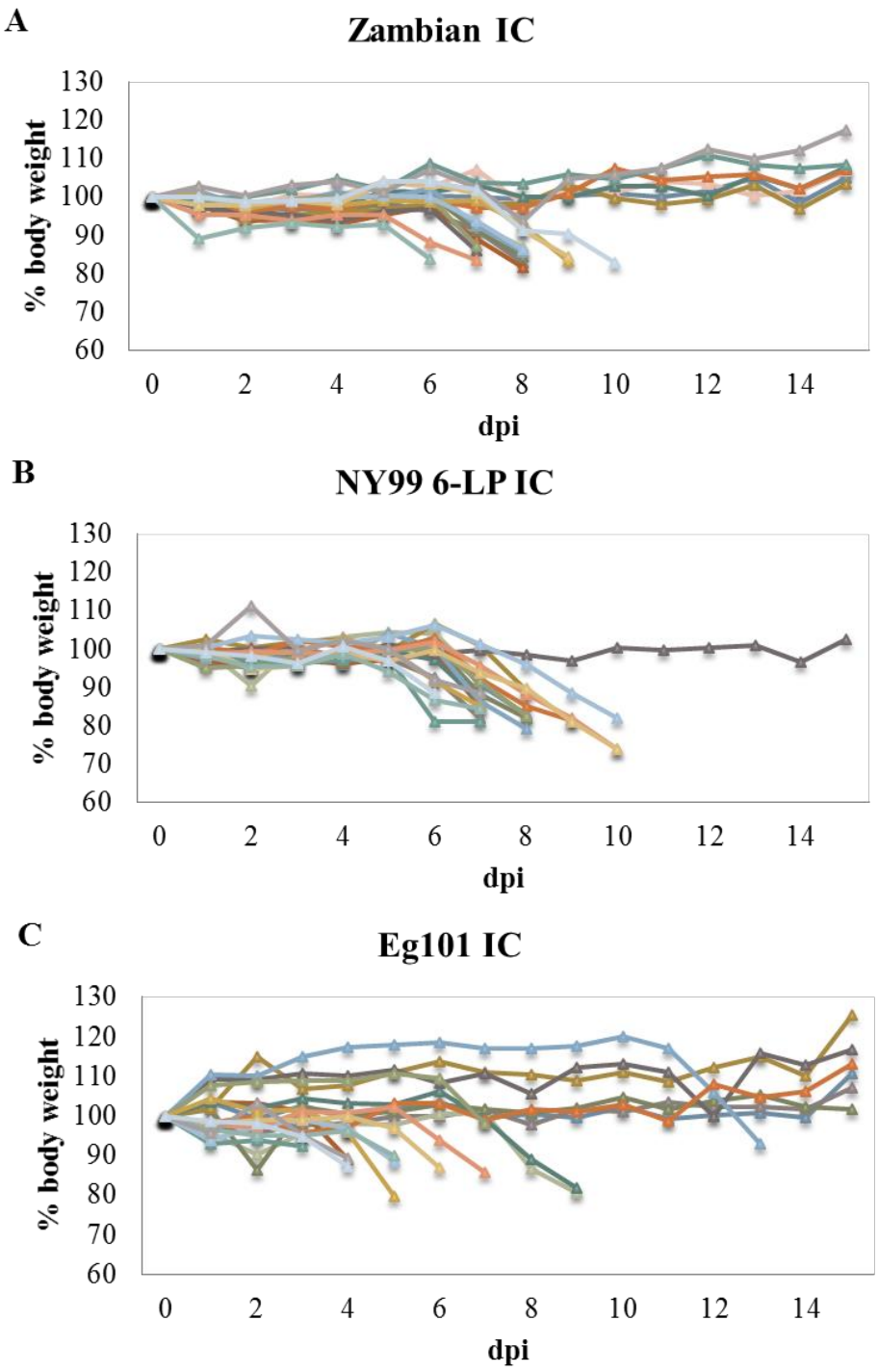

The body weight change of each mouse inoculated with WNV strain by IC method

Each WNV strain, including Zambian isolate (A), NY99 6-LP strain (B) or Eg101 strain (C) (1 PFU/mouse) was inoculated with IC method.

Table 1

Route of injection	Strain	Median survival time (dpi)
IP	Zambian isolate	10
	NY99 6-LP	10
	Eg101	11
IC	Zambian isolate	10
	NY99 6-LP	8
	Eg101	8

Median survival time of mice inoculated with each WNV strain

Discussion

Survival rate of mice inoculated with Zambian isolate through IP method was 5% (n=20) which was lower than those of high-pathogenic NY99 6-LP strain-inoculated mice (25%, n=20) and low-pathogenic Eg101 strain-inoculated mice (40%, n=20) (Fig. 11). In addition, the mice inoculated with Zambian isolate by IC method also demonstrated similar survival rate (35%, n=20) as that of Eg101 strain-inoculated mice (26%, n=19), which were higher than that of NY99 6-LP strain-inoculated mice (5%, n=19).

These results suggested that Zambian isolate has relatively high virulence to inbred experimental mice (C57BL/6JCr Slc) after IP method. However, the viral titer in brain after IP inoculation with Zambian isolate was much lower than those in brain after inoculation with NY99 6-LP or Eg101 strain (Fig. 13). It thus possible that the ability to pass through BBB or replicate in neurons of Zambian isolate is limited compared to NY99 and Eg101. Interestingly, the viral titer in brain tissue was not correlated with relatively high mortality in mice inoculated with Zambian isolate by the IP method. It is hypothesized that Zambian isolate also may induce high production of cytokines related to innate immune response, causing inflammation, and the immune response might result in high mortality in mice and low viral titer in the brain of inoculated-mice.

Relatively high mortality after inoculation of Zambian isolate may be related to infection and injury of other visceral organs rather than infection and inflammation of brain. Previous study reported that inoculation of SA93/01 (SPU93/01) strain disturbed autonomic nervous system due to infection and injury of brainstem and mid-cervical spinal cord, resulting in suppression of function of diaphragm, heart rate

viability and gastrointestinal stasis (Williams et al., 2015), In addition, it has been reported that another South African strain, SPU116/89, which was isolated from human patient with necrotic hepatitis. This strain also caused fatal hepatitis in experimental mice. According to phylogenetic classification, Zambian isolate was genetically close to these two strains (Fig. 10). It thus possible that the pathogenesis of relatively high mortality observed in Zambian isolate inoculated-C57BL/6 mice might be similar to that of either SA93/01 or SPU116/89 strain. Therefore, it is necessary to measure pro-inflammatory and inflammatory cytokines in mice and to examine other visceral organs after inoculation with Zambian isolate. These experiments are now ongoing.

The MST of mice after inoculation of each WNV strain by IP method was almost similar (Table 1, 10-11 dpi). Meanwhile, the MST of mice inoculated with Zambian isolate by IC method (11 dpi) was slightly longer than those of NY99- and Eg101 strain-inoculated mice (8 dpi). These results suggested that the virulence of Zambian strain after IC inoculation was relatively weaker than that of NY99 and Eg101 strain.

The affected mice after inoculation of Zambian isolate showed loss of body weight, ruffled fur, swollen eyes and neurological signs such as flaccid paralysis and disorientation. Additionally, the viral titers were detectable in brain samples at 6 and 9 dpi with Zambian isolate by IP method. These results indicated that Zambian isolate may have an ability to replicate in the body and pass through the BBB to reach to the brain in inbred experimental mice (C57BL/6JCr Slc). *In vitro* experiment using human neuroblastoma SK-N-SH cells demonstrated that Zambian isolate was able to replicate in neuronal cells as well as NY99 and Eg101 strains (data not shown). To examine the mechanism of mortality of experimental inbred mice after inoculation of

Zambian isolate, the pathological changes of brain and other organs induced by infection of Zambian isolate should be elucidated by immunohistopathological methods.

The present study indicated that Zambian isolate causes mortality in experimental inbred mice (C57BL/6JCr Slc) after IP or IC inoculation. This WNV isolate may cause fatal disease in human and other animals. Therefore, the WNV Zambian isolate should be concerned for a cause of unknown febrile illness and encephalitis in human and other animals in Zambia and neighbor countries.

Summary

Recently, a novel WNV was firstly isolated in the Republic of Zambia by our research group. The Zambian isolate was genetically close to lineage 2, South African strain, which is neuroinvasive and causes disease in human. However, the pathogenicity of the Zambian isolate has not been evaluated yet. The present study examined the *in vivo* effect of Zambian isolate in experimental inbred mice (C57BL/6JCr Slc). The mice were inoculated with Zambian isolate WNV strain either by IP or IC inoculation methods and compared with high-pathogenic NY99 6-LP and low-pathogenic Eg101 strains. Inoculation of Zambian isolate by IP method caused relatively high morbidity and mortality in the mice and the viral titer was detected in brain at 6 and 9 dpi. Interestingly, even though the Zambian isolate caused high mortality after IP injection as similar as the high pathogenic NY99 6-LP strain, the viral titer detected in brain tissue was much lower than those in NY99 6-LP- and Eg101- inoculated mice.

The precise pathogenicity of Zambian isolate WNV strain needs to be further investigated.

Conclusions

WNV was firstly isolated in 1937, the virus has been continuing a problem in public health in both developed and developing countries. Approved WNV vaccine for human is not available yet. Control of WNV is still difficult issue because this virus is mosquito-borne disease. Understanding of pathogenesis of WNV is necessary for development of therapeutic drug for treatment and vaccine for prevention of WNV infection. This thesis is divided into two chapters.

In chapter I, the role of VCP in WNV infection was investigated. It is suggested that VCP is important for WNV infection. Perturbation of VCP significantly suppressed WNV replication through inhibition of WNV genomic RNA replication and early steps of WNV intracellular replication cycle. The VCP might be promising target for development of WNV infection by targeting multiple stages of WNV life cycle.

In chapter II, the virulence of a novel strain of WNV isolated from mosquitoes captured in Zambia was evaluated by inoculation to the experimental inbred mice. The virulence of the Zambian isolate was compared to high-pathogenic strain, NY99 6-LP and low-pathogenic strain, Eg101. According to the obtained results, Zambian isolate caused relatively high morbidity and mortality in C57BL/6 mice after IP inoculation. The precise mechanism of Zambian isolate caused fatality in mice is now under investigation. This virus should be concerned as one of the causes of febrile diseases and encephalitis in human and other animals in Zambia and neighbor countries.

Acknowledgements

My deeply gratitude go first to my Professor. Hirofumi Sawa. I would like to appreciate him for his supervision both academic and general living entire all of my PhD life in Hokkaido University. His guidance is encouraging and contributing me to be good scientific researcher. I also thank for his kindness and warmth that could comfort me and let me pass the difficult time during PhD life. I would like to thank all of my committee members: Professor Ayato Takada, Dr. Kentaro Yoshii and Dr. Yasuko Orba for their valuables comments and suggestions. I would like to deeply express the gratitude to Dr. Shintaro Kobayashi for his precious guidance for research and life in Japan during this four and half years. He was not only research tutor, but also best friend and brother. I also would like to appreciate Dr. Michihito Sasaki and his family for suggestions, warmth and kindness. Sharing time with his family encouraged me and energized me to complete my PhD. I give big thanks to Dr. Paulina Duhita Anindita, the best friend in my PhD life. I appreciate her for support and sharing both academic and personal life. I would like to appreciate Dr. Micheal Carr for kindly proofing for my English. I thank all of laboratory members for support and giving suggestion and sharing good time together.

I would like to express my gratitude to all professors and staffs in the Graduate School of Veterinary Medicine, Research Center for Zoonosis Control and leading program office for help and support entire my doctoral study.

I would also like to appreciate my friends both Thai and International friends for help and encouragement. I would like to thank to my family whom I shared my life with. I would like to deeply gratitude to my mother for good education and taking care of me since I was born until the present.

Finally, I am grateful for funding support by The Ministry of Education,

Cultures, Sports, Sciences and Technology, Japan, that granted me for doctoral study.

References

Ambrose, R.L., Mackenzie, J.M., 2011. West Nile virus differentially modulates theunfolded protein response to facilitate replication and immune evasion. J.Virol. 85 (6), 2723–2732.

Arita, M., Wakita, T., Shimizu, H., 2012. Valosin-containing protein (VCP/p97) is required for poliovirus replication and is involved in cellular protein secretion pathway in poliovirus infection. J Virol 86(10), 5541-5553.

Bogachek, M.V., Zaitsev, B.N., Sekatskii, S.K., Protopopova, E.V., Ternovoi, V.A.,Ivanova, A.V., Kachko, A.V., Ivanisenko, V.A., Dietler, G., Loktev, V.B., 2010.Characterization of glycoprotein E C-end of West Nile virus and evaluation ofits interaction force with alphaVbeta3 integrin as putative cellular receptor.Biochemistry (Mosc) 75 (4), 472–480.

Bondre, V.P., Jadi, R.S., Mishra, A.C., Yergolkar, P.N., Arankalle, V.A., 2007. West Nile virus isolates from India: evidence for a distinct genetic lineage. J Gen Virol 88(Pt 3), 875-884.

Brinton, M.A., 2014. Replication cycle and molecular biology of the West Nile virus.Viruses 6 (1), 13–53.

Buchan, J.R., Kolaitis, R.M., Taylor, J.P., Parker, R., 2013. Eukaryotic stress granulesare cleared by autophagy and Cdc48/VCP function. Cell 153 (7), 1461–1474.

Bug, M., Meyer, H., 2012. Expanding into new markets–VCP/p97 in endocytosisand autophagy. J. Struct. Biol. 179 (2), 78–82.

Carnec, X., Meertens, L., Dejarnac, O., Perera-Lecoin, M., Hafirassou, M.L., Kitaura, J.,Ramdasi, R., Schwartz, O., Amara, A., 2016. The phosphatidylserine

andphosphatidylethanolamine receptor CD300a binds dengue virus and enhancesinfection. J. Virol. 90 (1), 92–102.

Centers for Disease Control and Prevention (CDC), 2016.West Nile virus disease cases and deaths reported to CDC by year and clinical presentation, 1999-2015. Available at: http:// www. cdc. gov. (accessed 18.08.16).

Chahar, H.S., Chen, S., Manjunath, N., 2013. P-body components LSM1, GW182,DDX3, DDX6 and XRN1 are recruited to WNV replication sites and positivelyregulate viral replication. Virology 436 (1), 1–7.

Chou, T.F., Deshaies, R.J., 2011. Quantitative cell-based protein degradation assays to identify and classify drugs that target the ubiquitin-proteasome system. J Biol Chem 286(19), 16546-16554.

Chu, J.J., Ng, M.L., 2004. Infectious entry of West Nile virus occurs through aclathrin-mediated endocytic pathway. J. Virol. 78 (19), 10543–10555.

Chu, J.J., Leong, P.W., Ng, M.L., 2006. Analysis of the endocytic pathway mediatingthe infectious entry of mosquito-borne flavivirus West Nile into Aedesalbopictus mosquito (C6/36) cells. Virology 349 (2), 463–475.

Courtney, S.C., Scherbik, S.V., Stockman, B.M., Brinton, M.A., 2012. West nile virusinfections suppress early viral RNA synthesis and avoid inducing the cell stressgranule response. J. Virol. 86 (7), 3647–3657.

Dargemont, C., Ossareh-Nazari, B., 2012. Cdc48/p97, a key actor in the interplaybetween autophagy and ubiquitin/proteasome catabolic pathways. Biochim.Biophys. Acta 1823 (1), 138–144.

Dauphin, G., Zientara, S., Zeller, H., Murgue, B., 2004. West Nile: worldwide currentsituation in animals and humans. Comp. Immunol. Microbiol. Infect. Dis. 27(5), 343–355.

Davis, C.W., Nguyen, H.Y., Hanna, S.L., Sánchez, M.D., Doms, R.W., Pierson, T.C.,2006. West Nile virus discriminates between DC-SIGN and DC-SIGNR forcellular attachment and infection. J. Virol. 80 (3), 1290–1301.

Denizot, M., Neal, J.W., Gasque, P., 2012. Encephalitis due to emerging viruses: CNSinnate immunity and potential therapeutic targets. J. Infect. 65 (1), 1–16.

Egberink, H., Addie, D.D., Boucraut-Baralon, C., Frymus, T., Gruffydd-Jones, T.,Hartmann, K., Horzinek, M.C., Hosie, M.J., Marsilio, F., Lloret, A., Lutz, H.,Pennisi, M.G., Radford, A.D., Thiry, E., Truyen, U., Möstl, K., Diseases, E.A.B.o.C.,2015. West Nile virus infection in cats: ABCD guidelines on prevention andmanagement. J. Feline Med. Surg. 17 (7), 617–619.

Fernandez-Garcia, M.D., Meertens, L., Bonazzi, M., Cossart, P., Arenzana-Seisdedos, F., Amara, A., 2011. Appraising the roles of CBLL1 and the ubiquitin/proteasome system for flavivirus entry and replication. J Virol 85(6), 2980-2989.

Gamino, V., Escribano-Romero, E., Blázquez, A.B., Gutiérrez-Guzmán, A.V.,Martín-Acebes, M., Saiz, J.C., Höfle, U., 2016. Experimental north american westnile virus infection in the red-legged partridge (Alectoris rufa). Vet. Pathol. 53(3), 585–593.

Gilfoy, F., Fayzulin, R., Mason, P.W., 2009. West Nile virus genome amplificationrequires the functional activities of the proteasome. Virology 385 (1), 74–84.

Gillespie, L.K., Hoenen, A., Morgan, G., Mackenzie, J.M., 2010. The endoplasmicreticulum provides the membrane platform for biogenesis of the flavivirusreplication complex. J. Virol. 84 (20), 10438–10447.

Hasebe, R., Suzuki, T., Makino, Y., Igarashi, M., Yamanouchi, S., Maeda, A., Horiuchi, M., Sawa, H., Kimura, T., 2010. Transcellular transport of West Nile virus-like particles across human endothelial cells depends on residues 156 and 159 of envelope protein. BMC Microbiol 10, 165.

Heinz, F.X., Allison, S.L., 2000. Structures and mechanisms in flavivirus fusion. Adv.Virus Res. 55, 231–269.

Hernández-Triana, L.M., Jeffries, C.L., Mansfield, K.L., Carnell, G., Fooks, A.R., Johnson, N., 2014. Emergence of west nile virus lineage 2 in europe: a review on the introduction and spread of a mosquito-borne disease. Front Public Health 2, 271.

Jiang, D., Weidner, J.M., Qing, M., Pan, X.B., Guo, H., Xu, C., Zhang, X., Birk, A., Chang, J., Shi, P.Y., Block, T.M., Guo, J.T., 2010. Identification of five interferon-induced cellular proteins that inhibit west nile virus and dengue virus infections. J Virol 84(16), 8332-8341.

Kaufmann, B., Rossmann, M.G., 2011. Molecular mechanisms involved in the early steps of flavivirus cell entry. Microbes Infect 13(1), 1-9.

Kaufusi, P.H., Kelley, J.F., Yanagihara, R., Nerurkar, V.R., 2014. Induction ofendoplasmic reticulum-derived replication-competent membrane structuresby West Nile virus non-structural protein 4B. PLoS One 9 (1), e84040.

Kimura, T., Kimura-Kuroda, J., Nagashima, K., Yasui, K., 1994. Analysis of virus-cell binding characteristics on the determination of Japanese encephalitis virus susceptibility. Arch Virol 139(3-4), 239-251.

Knipe, D. M. Howley, P. M., Cohen, J. I., Griffin, D. E., Lamb, R. A., Martin, M. A., Racaniello, V. R., Roizman, B. Fields Virology 6th edition. Philadelphia; Lippincott Williams & Wilkins. 2013.

Kobayashi, S., Orba, Y., Yamaguchi, H., Kimura, T., Sawa, H., 2012. Accumulation of ubiquitinated proteins is related to West Nile virus-induced neuronal apoptosis. Neuropathology 32(4), 398-405.

Kobayashi, S., Suzuki, T., Igarashi, M., Orba, Y., Ohtake, N., Nagakawa, K., Niikura, K., Kimura, T., Kasamatsu, H., Sawa, H., 2013. Cysteine residues in the major capsid protein, Vp1, of the JC virus are important for protein stability and oligomer formation. PLoS One 8(10), e76668.

Kobayashi, S., Orba, Y., Yamaguchi, H., Takahashi, K., Sasaki, M., Hasebe, R., Kimura, T., Sawa, H., 2014. Autophagy inhibits viral genome replication and gene expression stages in West Nile virus infection. Virus Res 191, 83-91.

Kobayashi, S., Suzuki, T., Kawaguchi, A., Phongphaew, W., Yoshii, K., Iwano, T., Harada, A., Kariwa, H., Orba, Y., Sawa, H., 2016. Rab8b regulates transport of West Nile virus particles from recycling endosomes. J Biol Chem 291(12), 6559-6568.

Kobayashi, S., Yoshii, K., Hirano, M., Muto, M., Kariwa, H., 2017. A novel reverse genetics system for production of infectious West Nile virus using homologous recombination in mammalian cells. J Virol Methods 240:14-20.

Koller, K.J., Brownstein, M.J., 1987. Use of a cDNA clone to identify a supposedprecursor protein containing valosin. Nature 325 (6104), 542–545.

Kramer, L.D., Bernard, K.A., 2001. West Nile virus infection in birds and mammals.Ann. N. Y. Acad. Sci. 951, 84–93.

Krishnan, M.N., Ng, A., Sukumaran, B., Gilfoy, F.D., Uchil, P.D., Sultana, H., Brass, A.L., Adametz, R., Tsui, M., Qian, F., Montgomery, R.R., Lev, S., Mason, P.W., Koski, R.A., Elledge, S.J., Xavier, R.J., Agaisse, H., Fikrig, E., 2008. RNA interference screen for human genes associated with West Nile virus infection. Nature 455(7210), 242-245.

Kumar, M., Verma, S., Nerurkar, V.R., 2010. Pro-inflammatory cytokines derived from West Nile virus (WNV)-infected SK-N-SH cells mediate neuroinflammatory markers and neuronal death. J Neuroinflammation 7, 73.

Kumar, M., Belcaid, M., Nerurkar, V.R., 2016. Identification of host genes leading to West Nile virus encephalitis in mice brain using RNA-seq analysis. Sci Rep 6:26350.

Lichtensteiger, C.A., Heinz-Taheny, K., Osborne, T.S., Novak, R.J., Lewis, B.A., Firth,M.L., 2003. West Nile virus encephalitis and myocarditis in wolf and dog.Emerg. Infect. Dis. 9 (10), 1303–1306.

Ma, H., Dang, Y., Wu, Y., Jia, G., Anaya, E., Zhang, J., Abraham, S., Choi, J.G., Shi, G., Qi,L., Manjunath, N., Wu, H., 2015. A CRISPR-based screen identifies genesessential for West-Nile-virus-induced cell death. Cell Rep. 12 (4), 673–683.

Magurano, F., Remoli, M.E., Baggieri, M., Fortuna, C., Marchi, A., Fiorentini, C., Bucci, P., Benedetti, E., Ciufolini, M.G., Rizzo, C., Piga, S., Salcuni, P., Rezza, G., Nicoletti, L., 2012. Circulation of West Nile virus lineage 1 and 2 during an outbreak in Italy. Clin Microbiol Infect 18(12), E545-547.

Martina, B.E., Koraka, P., van den Doel, P., Rimmelzwaan, G.F., Haagmans, B.L.,Osterhaus, A.D., 2008. DC-SIGN enhances infection of cells with glycosylatedWest Nile virus in vitro and virus replication in human dendritic

cells inducesproduction of IFN-alpha and TNF-alpha. Virus Res. 135 (1), 64–71.

Makino, Y., Suzuki, T., Hasebe, R., Kimura, T., Maeda, A., Takahashi, H., Sawa, H., 2014. Establishment of tracking system for West Nile virus entry and evidence of microtubule involvement in particle transport. J Virol Methods 195, 250-257.

Maric, M., Maculins, T., De Piccoli, G., Labib, K., 2014. Cdc48 and a ubiquitin ligase drive disassembly of the CMG helicase at the end of DNA replication. Science 346(6208), 1253596.

Meyer, H., Bug, M., Bremer, S., 2012. Emerging functions of the VCP/p97 AAA-ATPase in the ubiquitin system. Nat Cell Biol 14(2), 117-123.

Meyer, H., Weihl, C.C., 2014. The VCP/p97 system at a glance: connecting cellular function to disease pathogenesis. J Cell Sci 127(Pt 18), 3877-3883.

Morizono, K., Chen, I.S., 2014. Role of phosphatidylserine receptors in envelopedvirus infection. J. Virol. 88 (8), 4275–4290.

Mweene-Ndumba, I., Siziya, S., Monze, M., Mazaba, M.L., Masaninga, F., Songolo, P., Mwaba, P., Babaniyi, O.A., 2015. Seroprevalence of West Nile Virus specific IgG and IgM antibodies in North-Western and Western provinces of Zambia. Afr Health Sci 15(3), 803-809.

Orba, Y., Hang'ombe, B.M., Mweene, A., Wada, Y., Anindita, P.D., Phongphaew, W., Qui.Y., Kajihara, M., Kajihara, A.M., Eto, Y., Sasaki, M., Hall, W.W., Eshita, Y., Sawa, H., 2017. First isolation of West Nile virus in Zambia from mosquitoes. (in submission)

Panda, D., Rose, P.P., Hanna, S.L., Gold, B., Hopkins, K.C., Lyde, R.B., Marks, M.S.,Cherry, S., 2013. Genome-wide RNAi screen identifies SEC61A and

VCP asconserved regulators of Sindbis virus entry. Cell Rep. 5 (6), 1737–1748.

Paz, S., 2015. Climate change impacts on West Nile virus transmission in a globalcontext. Philos. Trans. R. Soc. Lond. B Biol. Sci. 370 (1665).

Perera-Lecoin, M., Meertens, L., Carnec, X., Amara, A., 2014. Flavivirus entryreceptors: an update. Viruses 6 (1), 69–88.

Pye, V.E., Dreveny, I., Briggs, L.C., Sands, C., Beuron, F., Zhang, X., Freemont, P.S.,2006. Going through the motions: the ATPase cycle of p97. J. Struct. Biol. 156(1), 12–28.

Ramanathan, H.N., Ye, Y., 2012. The p97 ATPase associates with EEA1 to regulatethe size of early endosomes. Cell Res. 22 (2), 346–359.

Read, R.W., Rodriguez, D.B., Summers, B.A., 2005. West Nile virus encephalitis in adog. Vet. Pathol. 42 (2), 219–222.

Ritz, D., Vuk, M., Kirchner, P., Bug, M., Schütz, S., Hayer, A., Bremer, S., Lusk, C.,Baloh, R.H., Lee, H., Glatter, T., Gstaiger, M., Aebersold, R., Weihl, C.C., Meyer, H.,2011. Endolysosomal sorting of ubiquitylated caveolin-1 is regulated by VCPand UBXD1 and impaired by VCP disease mutations. Nat. Cell Biol. 13 (9),1116–1123.

Panda, D., Rose, P.P., Hanna, S.L., Gold, B., Hopkins, K.C., Lyde, R.B., Marks, M.S., Cherry, S., 2013. Genome-wide RNAi screen identifies SEC61A and VCP as conserved regulators of Sindbis virus entry. Cell Rep 5(6), 1737-1748.

Plevka, P., Battisti, A.J., Sheng, J., Rossmann, M.G., 2014. Mechanism formaturation-related reorganization of flavivirus glycoproteins. J. Struct. Biol.185 (1), 27–31.

Ramanathan, H.N., Ye, Y., 2012. The p97 ATPase associates with EEA1 to regulatethe size of early endosomes. Cell Res. 22 (2), 346–359.

Roby, J.A., Setoh, Y.X., Hall, R.A., Khromykh, A.A., 2015. Post-translationalregulation and modifications of flavivirus structural proteins. J. Gen. Virol. 96(Pt 7), 1551–1569.

Samuel, M.A., Diamond, M.S., 2006. Pathogenesis of West Nile Virus infection: abalance between virulence, innate and adaptive immunity, and viral evasion. J.Virol. 80 (19), 9349–9360.

Scholle, F., Girard, Y.A., Zhao, Q., Higgs, S., Mason, P.W., 2004. trans-Packaged West Nile virus-like particles: infectious properties in vitro and in infected mosquito vectors. J Virol 78(21), 11605-11614.

Seguin, S.J., Morelli, F.F., Vinet, J., Amore, D., De Biasi, S., Poletti, A., Rubinsztein,D.C., Carra, S., 2014. Inhibition of autophagy, lysosome and VCP functionimpairs stress granule assembly. Cell Death Differ. 21 (12), 1838–1851.

Shimojima, M., Takenouchi, A., Shimoda, H., Kimura, N., Maeda, K., 2014. Distinctusage of three C-type lectins by Japanese encephalitis virus: DC-SIGN,DC-SIGNR, and LSECtin. Arch. Virol 159 (8), 2023–2031.

Shirato, K., Kimura, T., Mizutani, T., Kariwa, H., Takashima, I., 2004a. Different chemokine expression in lethal and non-lethal murine West Nile virus infection. J Med Virol 74(3), 507-513.

Shirato, K., Miyoshi, H., Goto, A., Ako, Y., Ueki, T., Kariwa, H., Takashima, I., 2004b. Viral envelope protein glycosylation is a molecular determinant of the neuroinvasiveness of the New York strain of West Nile virus. J Gen Virol 85(Pt 12), 3637-3645.

Smit, J.M., Moesker, B., Rodenhuis-Zybert, I., Wilschut, J., 2011. Flavivirus cell entryand membrane fusion. Viruses 3 (2), 160–171.

Smithburn, K.C., Hughes, T.P., Burke, A.W., Paul, J.H., 1940. A Neurotropic VirusIsolated from the Blood of a Native of Uganda. Am. J. Trop. Med. Hyg. s1–20(20), 471–492.

Stolz, A., Hilt, W., Buchberger, A., Wolf, D.H., 2011. Cdc48: a power machine inprotein degradation. Trends Biochem. Sci. 36 (10), 515–523.

Suthar, M.S., Diamond, M.S., Gale, M., 2013. West Nile virus infection andimmunity. Nat. Rev. Microbiol. 11 (2), 115–128.

Takada, A., Ebihara, H., Feldmann, H., Geisbert, T.W., Kawaoka, Y., 2007. Epitopes required for antibody-dependent enhancement of Ebola virus infection. J Infect Dis 196 Suppl 2, S347-356.

Takahashi, H., Ohtaki, N., Maeda-Sato, M., Tanaka, M., Tanaka, K., Sawa, H., Ishikawa, T., Takamizawa, A., Takasaki, T., Hasegawa, H., Sata, T., Hall, W.W., Kurata, T., Kojima, A., 2009. Effects of the number of amino acid residues in the signal segment upstream or downstream of the NS2B-3 cleavage site on production and secretion of prM/M-E virus-like particles of West Nile virus. Microbes Infect 11(13), 1019-1028.

Troupin, A., Colpitts, T.M., 2016. Overview of west nile virus transmission andepidemiology. Methods Mol. Biol. 1435, 15–18.

Venter, M., Swanepoel, R., 2010. West Nile virus lineage 2 as a cause of zoonotic neurological disease in humans and horses in southern Africa. Vector Borne Zoonotic Dis 10(7), 659-664.

Verma, R., Oania, R., Fang, R., Smith, G.T., Deshaies, R.J., 2011. Cdc48/p97 mediates UV-dependent turnover of RNA Pol II. Mol Cell 41(1), 82-92.

Wang, Q., Li, L., Ye, Y., 2008. Inhibition of p97-dependent protein degradation by Eeyarestatin I. J Biol Chem 283(12), 7445-7454.

Wang, Q., Shinkre, B.A., Lee, J.G., Weniger, M.A., Liu, Y., Chen, W., Wiestner, A., Trenkle, W.C., Ye, Y., 2010. The ERAD inhibitor Eeyarestatin I is a bifunctional compound with a membrane-binding domain and a p97/VCP inhibitory group. PLoS One 5(11), e15479.

Welsch, S., Miller, S., Romero-Brey, I., Merz, A., Bleck, C.K., Walther, P., Fuller, S.D.,Antony, C., Krijnse-Locker, J., Bartenschlager, R., 2009. Composition andthree-dimensional architecture of the dengue virus replication and assemblysites. Cell Host Microbe 5 (4), 365–375.

Wilcox, A.J., Laney, J.D., 2009. A ubiquitin-selective AAA-ATPase mediates transcriptional switching by remodelling a repressor-promoter DNA complex. Nat Cell Biol. 11(12):1481-1486.

Williams, J.H., Mentoor, J.D., Van Wilpe, E., Venter, M., 2015. Comparative pathology of neurovirulent lineage 1 (NY99/385) and lineage 2 (SPU93/01) West Nile virus infections in BALBc mice. Vet Pathol 52(1), 140-151.

Wolf, D.H., Stolz, A., 2012. The Cdc48 machine in endoplasmic reticulum associatedprotein degradation. Biochim. Biophys. Acta 1823 (1), 117–124.

Wong, H.H., Kumar, P., Tay, F.P., Moreau, D., Liu, D.X., Bard, F., 2015. Genome-Wide Screen Reveals Valosin-Containing Protein Requirement for Coronavirus Exit from Endosomes. J Virol 89(21), 11116-11128.

Xia, D., Tang, W.K., Ye, Y., 2016. Structure and function of the AAA+ ATPasep97/Cdc48p. Gene 583 (1), 64–77.

Yamanaka, K., Sasagawa, Y., Ogura, T., 2012. Recent advances in p97/VCP/Cdc48 cellular functions. Biochim Biophys Acta 1823(1), 130-137.

Yi, Z., Fang, C., Zou, J., Xu, J., Song, W., Du, X., Pan, T., Lu, H., Yuan, Z., 2016. Affinity Purification of the Hepatitis C Virus Replicase Identifies Valosin-Containing Protein, a Member of the ATPases Associated with Diverse Cellular Activities Family, as an Active Virus Replication Modulator. J Virol 90(21), 9953-9966.

Yu, I.M., Zhang, W., Holdaway, H.A., Li, L., Kostyuchenko, V.A., Chipman, P.R., Kuhn,R.J., Rossmann, M.G., Chen, J., 2008. Structure of the immature dengue virus atlow pH primes proteolytic maturation. Science 319 (5871), 1834–1837.

Zaitsev, B.N., Benedetti, F., Mikhaylov, A.G., Korneev, D.V., Sekatskii, S.K., Karakouz,T., Belavin, P.A., Netesova, N.A., Protopopova, E.V., Konovalova, S.N., Dietler, G.,Loktev, V.B., 2014. Force-induced globule-coil transition in laminin bindingprotein and its role for viral-cell membrane fusion. J. Mol. Recognit. 27 (12),727–738.

Zidane, N., Ould-Abeih, M.B., Petit-Topin, I., Bedouelle, H., 2013. The folded anddisordered domains of human ribosomal protein SA have both idiosyncraticand shared functions as membrane receptors. Biosci. Rep. 33 (1), 113–124.

Zhong, X., Pittman, R.N., 2006. Ataxin-3 binds VCP/p97 and regulatesretrotranslocation of ERAD substrates. Hum. Mol. Genet. 15 (16), 2409–2420.